BBA - Molecular Cell Research 1869 (2022) 119342

Contents lists available at ScienceDirect

BBA - Molecular Cell Research

journal homepage: www.elsevier.com/locate/bbamcr

Research Paper

Multiple checkpoints of protein clearance machinery are modulated by a common microRNA, miR-4813-3p, through its putative target genes: Studies employing transgenic *C. elegans* model

Arunabh Sarkar [a], Shamsuzzama [a], Lalit Kumar [a], Rohil Hameed [a,b], Aamir Nazir [a,b,*]

[a] Division of Neuroscience and Ageing Biology, CSIR-Central Drug Research Institute, Lucknow, UP, India
[b] Academy of Scientific and Innovative Research (AcSIR), Ghaziabad 201002, India

ARTICLE INFO

Keywords:
Neurodegenerative diseases (NDs)
Parkinson's Disease (PD)
Protein Quality Control (PQC)
Unfolded Protein Response (UPR)

ABSTRACT

In order to maintain cellular homeostasis and a healthy state, aberrant and aggregated proteins are to be recognized and rapidly cleared from cells. Parkinson's disease, known to be associated with multiple factors; presents with impaired clearance of aggregated alpha synuclein as a key factor. We endeavored to study microRNA molecules with potential role on regulating multiple checkpoints of protein quality control within cells. Carrying out global miRNA profiling in a transgenic *C. elegans* model that expresses human alpha synuclein, we identified novel miRNA, miR-4813-3p, as a significantly downregulated molecule. Further studying its putative downstream target genes, we were able to mechanistically characterize six genes *gbf-1, vha-5, cup-5, cpd-2, acs-1* and C27A12.7, which relate to endpoints associated with alpha synuclein expression, oxidative stress, locomotory behavior, autophagy and apoptotic pathways. Our study reveals the novel role of miR-4813-3p and provides potential functional characterization of its putative target genes, in regulating the various pathways associated with PQC network. miR-4813-3p modulates ER^{UPR}, MT^{UPR}, autophagosome-lysosomal-pathway and the ubiquitin-proteasomal-system, making this molecule an interesting target for further studies towards therapeutically addressing multifactorial aspect of Parkinson's disease.

1. Introduction

It is a widely accepted fact that accumulation of protein aggregates is one of the most crucial factors associated with disease progression and outcome of multifactorial neurodegenerative diseases (NDs). Structural stability and molecular partnerships of misfolded proteins are altered because of their exposure to internal domains and hence form toxic aggregates in Alzheimer's disease (AD; aggregation of amyloid beta) and Parkinson's disease (PD; aggregation of α-synuclein) [1].

To check, regulate and prevent protein accumulation, cells employ their own protein quality control system (PQC). Inside the cell via its quality control (QC) pathways, cells invariably check the protein molecules for occasional damage or errors. PQC machinery recognizes the aberrant protein and either corrects it or degrades it rapidly to maintain cellular homoeostasis [2,3]. Within the neuron internally, PQC occurs in almost every cellular compartment, which is a necessity to identify a wide range of defects in the protein molecule from mislocalization to misfolding. The errors in recognizing such targets by quality control manifest in the unwanted accumulation of faulty stock that may aggregate further and create deleterious consequences. On the other hand, over sensitive or unregulated recognition may unreasonably target the functional proteins for degradation, draining the key resource of the cell. Therefore, very high precision in PQC is required within the cell, and knowing what goes wrong during PD, can aid in better understanding of the disease and in developing effective therapeutic strategies against it [4–6].

Elimination of protein aggregates within the cell is broadly affected by the ubiquitin-proteasome system, chaperone-mediated autophagy, lysosomal associated autophagy, and unfolded protein response (UPR) pathway of the endoplasmic reticulum and mitochondria. Therefore, identifying a potential common trigger that can regulate the major degradation pathways of PQC, may aid in bettering the outcome of protein clearance, thus ameliorating disease related effects. Among discrete mechanistic triggers for protein expression, the miRNA molecules are considered mechanistically critical as these molecules regulate expression of multiple genes. miRNAs are evolutionarily conserved

* Corresponding author at: Division of Neuroscience and Ageing Biology, CSIR-Central Drug Research Institute, Lucknow 226031, Uttar Pradesh, India.
E-mail address: anazir@cdri.res.in (A. Nazir).

https://doi.org/10.1016/j.bbamcr.2022.119342
Received 7 June 2022; Received in revised form 14 August 2022; Accepted 17 August 2022
Available online 20 August 2022

nucleotides with a length of 20–25 base pairs; they block protein synthesis either by inhibiting the translation of mRNA or by degrading the mRNA itself. However, there are some reports which show they can even regulate gene expression at the transcription level [7,8].

In mammals, miRNAs play a crucial role in brain development, neuronal function, specification, and even in repair of maintenance system [9–11]. miRNAs also regulate most of the genes that are required for cellular identity, emphasizing their essential role in the maturation of cells, tissue, and organs [12,13]. Uncoordinated variations either in biogenesis or functioning of miRNAs have been found associated to manifest diverse ailments which includes neurodegenerative disease, cardiovascular disease, diabetes mellitus and cancer [14–16].

miRNAs have a discrete expression pattern, which not only varies from healthy to diseased individual but also from organ to organ within a particular organism. In present studies, we report a comparison of global miRNA profile of transgenic *C. elegans* strain expressing human α-synuclein (NL5901) in comparison to wild type strain (N2). We have successfully identified novel miRNA molecules that were not previously known to be associated with NDs. We further carried out in silico studies towards identifying their downstream predicted targets followed by their functional characterization and validation, having an association with the essential pathways of protein quality control. We suggest that if we can enhance the fidelity of PQC machinery by overexpressing crucial targets either genetically or pharmacologically, the clearance of aberrant and aggregating proteins could be a significant step towards slowing down the progression of NDs. Our studies present a considerable step towards identifying novel modulators of PQC machinery, which could be studied further for a targeted cure via bettering protein clearance in aberrant conditions.

2. Results

2.1. Potential miRNA molecules identified by global miRNA profiling in transgenic C. elegans model

We performed miRNA profiling of transgenic *C. elegans* model for PD, NL5901 (which expresses human α-synuclein protein tagged with YFP) in comparison to wild type strain (N2) employing Next Generation Sequencing (NGS) method. We have successfully identified novel miRNA molecules; among these, we found that miR-4813-3p is the most down-regulated molecule (>15-fold) and miR-8188-5p is the most upregulated molecule (>100 folds) as shown in Fig. 1A. The intriguing differential expression pattern of these two miRNAs was further validated by TaqMan assay, where miR-4813-3p was observed to exhibit 40-fold downregulation whereas miR-8188-5p exhibited a 9-fold upregulation (Fig. 1B). The 40-fold downregulation of miR-4813-3p inferred the importance of this molecule thus making it prudent to study it further in the context of PQC machinery.

In our preliminary studies, we prepared a dataset of predicted downstream mRNA targets of miR-4813-3p by using the miRbase towards getting its mature sequence and by using RNA22 tool to get the predicted targets; we identified 266 relevant targets (shown in Supplementary Table 2; excel sheet). Selective filters like (at least 60 % homology with the human counterparts, regulatory role in protein quality control or neuronal expressions based on existing literature mining) were applied to the dataset, and we ended up with 20 predicted downstream targets of miR-4813-3p, for which RNAi assays were available in the Ahringer library, as shown Table 1.

2.2. α-Synuclein expression gets modulated after knockdown of putative downstream targets of miR-4813-3p in transgenic C. elegans

Expression of α-synuclein followed by its accumulation being a key feature of PD [17,18], we studied the identified predicted downstream effector molecules of miR-4813-3p, for their role in accrual of α-synuclein NL5901 strain of *C. elegans*. We observed that from the 20 identified genes, RNAi of 12 *(acs-1, lgc-47, vha-5, B0361.6,* C27A12.7, D2030.2*, T09E8.3, cpd-2, gbf-1, nuo-5,* C05D11.9 and *cup-5*) significantly increases the accrual of α-synuclein and RNAi of 2 (*gpx-6* and *unc-11)* decreases accrual of α-synuclein, whereas RNAi of 6 genes (*cua-1, glr-1, egl-45,* C14C11.4*, lon-3, hke-1)* have been found to have no significant effect on accrual of α-synuclein, as shown in Fig. 2A and B. RNAi of *asc-1, cpd-2, cup-5* and *glr-1* induced a developmental delay as the worms were observed to attain L4 stage post 75 h of embryo isolation as shown in Fig. 3A and supplementary fig. 4.

2.3. Putative downstream targets of miR-4813-3p modulate multiple factors including α-synuclein accrual

The studies on α-synuclein accrual by knockdown of predicted targets of miR-4813-3p and further in silico interaction studies (using Gene Mania and STRING) revealed involvement of these predicted downstream targets in PD associated endpoints. We figured that the identified molecules may modulate multiple factors regulating biochemical pathways inside the cell like the protein quality control machinery, mitochondrial energy balance, muscle contraction, fatty acid metabolism, cytoskeletal dynamics, and calcium homeostasis (shown in Table 2) affecting other endpoints including α-synuclein accrual. These observations indicate, miR-4813-3p can regulate multiple pathways and probably can emerge as a common trigger for endpoints associated with PD. Based on our categorization and observed results, we observed that miR-4813-3p has six putative downstream targets (out of the 12, whose RNAi has increased the α-synuclein accrual) that can directly modulate the protein quality control machinery. To check further whether the expression pattern of these six PQC genes gets modulated by miR-4813-3p, we employed a knock out strain of miR-4813 (MLC425) and found there is significant increase in the mRNA levels of PQC genes shown in supplementary fig. 1 and supplementary table A. Hence, the six identified genetic modulators (*gbf-1, vha-5, cup-5, cpd-2, acs-1* & C27A12.7), presence of which seem to be critical for maintaining efficient protein quality control along with associated functions, were chosen for further functional characterization (reported function of PQC genes is described in Section 2.9 and Table 1).

We performed phenotypic studies in MLC425 (knock out strain of miR-4813) like body morphometry, fat content, locomotory and odorant response and behavioral assays which provide certain cues suggesting that miR-4813 might act upstream of PQC gene targets regulating α-synuclein accrual. We have observed, at all developmental stages that MLC425 shows a significant increase in its size as compared to wild type worms (N2) (supplementary fig. 3A), this might be probably because of marked increase in the fat content as observed under the knock out background of miR-4813 (supplementary fig. 3D). We further observed that in the absence of miR-4813, worms exhibit a significant increase in the locomotory behavior and quick response to both attractive and repellent odorant as compared to wild type (supplementary fig. 3B and Fig. 3C). Low fat deposition was previously reported to be associated with PD. It is known that the downregulated locomotory and odorant response time behavior is usually the phenotypic manifestation of distorted signaling of nigrostriatal pathway because of α-synuclein accumulation in the neurons.

2.4. Distorted dopamine signaling and locomotory behavior is observed after knockdown of putative downstream targets of miR-4813–3p

Death of nigrostriatal dopaminergic (DAergic) neurons is the dominant pathology of PD, resulting in a severe decrease of striatal dopamine levels. As age-associated functional decline is attributed to the failure of protein homeostasis in neurons [19–21], to know whether the knockdown of PQC genes impacts dopaminergic neuronal function, we carried out quantification of the dopamine levels by LC-MS in the transgenic strain of *C. elegans* NL5901. Interestingly, we observed a significant decrease in total dopamine content levels after the knockdown of PQC

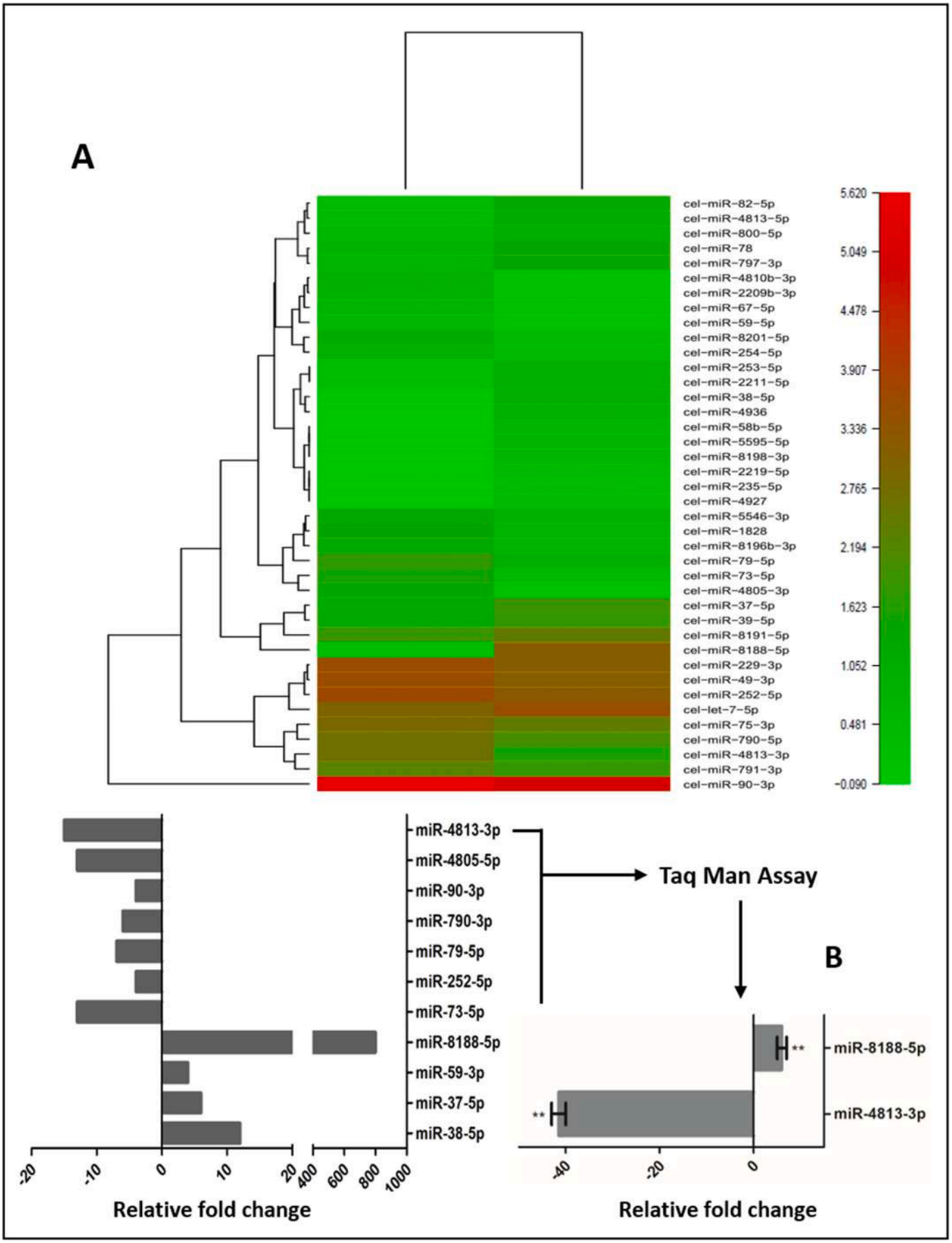

(caption on next page)

Fig. 1. Identification of specific miRNA from global miRNA profiling in NL5901: (A); The figure describes the NGS miRNA profile of transgenic *C. elegans* (NL5901) expressing human α-Synuclein in comparison to N2 wild type strain; expression profile is depicted in the heatmap, and fold-change of miRNAs plotted with the help of R-package where we have identified miR-8188-5p is the most upregulated one and miR-4813-3p is the most down-regulated one (B); Shows miRNAs fold change, studied through Taq man real-time PCR in NL5901. Graphical representation of miRNA fold change in a transgenic strain expressing human α-synuclein (NL5901) over wild type train (N2 Quantified by and non-parametric independent *t*-test (Mean ± SEM; $*p < 0.05$, $**p < 0.005$, $***p < 0.0005$ & ns: non-significant).

genes as shown in Fig. 3B and supplementary table B.

In both vertebrate and invertebrate various findings suggest that dopaminergic neurons play a very critical role in various adaptive behaviours for the survival. Dopaminergic neurons integrate sensory information in their earning behavior which helps them to make decisions. PD is also associated with defects in motor neuronal signaling which leads to motor behavior defects [22–25]. Along with the observed decline in the dopamine levels after RNAi of PQC genes, we studied the locomotory behavior in worms as total number of thrashes per minute, after silencing of PQC downstream targets. We observed a decrease in the mean thrashing count after knockdown of PQC genes (Fig. 3C and supplementary table C). It is known that in Parkinson's disease, the dopamine transporter (DAT-1) can be reduced by upto 50–70 %; therefore, the dopamine transporter alone can be a critical determinant of the dopamine availability in PD [26]. We studied the effect on dopamine transporter (DAT-1) after knockdown of predicted PQC downstream targets by employing a transgenic strain of *C. elegans* BZ555 (which expresses GFP under dat-1 promoter in all eight of its dopaminergic neurons). We observed a non-significant variation in DAT-1 expression levels after RNAi of predicted downstream targets (Fig. 3D) even though there were significantly low dopamine levels. This observation indicates that RNAi of PQC genes distorts dopamine signaling and locomotory behavior by decreasing the total dopamine content which reflects as reduced number of thrashing counts in the worm.

Table 1
List of predicted downstream targets of miR-4813-3p after applying selective filters.

S. No.	Common gene name	Sequence name	Role in *C. elegans*
1.	*vha-5*	F55H10.4	Encodes an orthologue of subunit a of the membrane-bound (V0) domain of vacuolar proton-translocating ATPase (V-ATPase).
2.	*hke-4.1*	T28F3.3	Predicted to have metal ion transmembrane transporter activity, and it is expressed in nervous system
3.	C27A12.7	C27A12.7	Predicted to have ubiquitin-protein transferase activity, based on protein domain information.
4.	D2030.2	D2030.2	involved in nematode larval development, receptor-mediated endocytosis and striated muscle myosin thick filament assembly.
5.	*acs-1*	F46E10.1	involved in apoptotic process, embryo development, growth, lipid storage, locomotion, nematode larval development and reproduction.
6.	T09E8.3	T09E8.3	cni-1 is expressed in the nervous system; cni-1 is localized to the endoplasmic reticulum and the synapse.
7.	*cua-1*	Y76A2A.2	When mutated leads to Hailey-Hailey disease; loss of cua-1 activity via RNAi results in a number of defects, including slow growth, uncoordinated or no locomotion, adult and larval lethality, and axon guidance abnormalities.
8.	*cpd-2*	T27A8.1	Have peptidases activity
9.	*lgc-47*	F47A4.1	Ion channel in neuron
10.	B0361.6	B0361.6	Receptor mediated endocytosis and it is expressed in nervous system
11.	*glr-1*	C06E1.4	Glutamate receptor and it is involved in memory function.
12.	*gbf-1*	C24H11.7	Involve in apoptotic process
13.	*egl-45*	C27D11.1	egl-45 is predicted to have translation regulator activity, based on sequence information; egl-45 is expressed in the nervous system.
14.	*cup-5*	R13A5.1	Required for normal degradation of lysosome
15.	C05D11.9	C05D11.9	Code for pop-1, a riboendonuclease in mitochondria, that cleave mitochondrial RNA
16.	*gpx-6*	T09A12.2	Glutathione peroxidase in neuron
17.	*unc-11*	C32E8.10	Regulates neurotransmitter release by controlling vesicle trafficking and fusion
18.	C14C11.4	C14C11.4	Involve in apoptotic process
19.	*nuo-5*	Y45G12B.1	NADH-Ubiquinone Oxidoreductase Fe—S PROTEIN 1, which when mutated leads to mitochondrial complex I deficiency.
20.	*lon-3*	ZK836.1	Acetyl choline esterase

Source: Worm base version: WS275.

2.5. Expression of autophagy and apoptotic genes gets altered after knockdown of predicted PQC targets of miR-4813-3p

The clearance of protein aggregates and damaged organelles are mainly associated with autophagy. Mutations and downregulation of autophagy related genes are well known to be correlated with PD [27–32]. In order to study whether these putative PQC targets have any involvement in autophagy (the main protein clearance machinery of the cell) we studied known autophagy marker genes (*bec-1, lgg-1, atg-5 & vps-34*) using the quantitative real-time PCR (qPCR) method under the knockdown condition of PQC genes. We observed that RNAi of each PQC target leads to the downregulation of marker genes, as shown in Fig. 4A and supplementary table D and E. *bec-1* plays an essential role in the functioning of class III PI3 kinase LET-512; it is a crucial protein required for autophagy, endocytosis, and membrane trafficking. *lgg-1* encodes the ortholog of mammalian MAP-LC3 required for degradation of cellular components. *atg-5* is involved in autophagosome assembly during the autophagy process. *vps-34* encodes an ortholog of the phosphoinositide 3-kinase and is required for vesicular trafficking, including autophagy and apoptotic cell clearance [33–35].

As we observed a significant decrease in the mRNA expression pattern of autophagy-related gene *lgg-1* after RNAi of predicted PQC downstream targets, we have further studied autophagosome vesicle formation employing a transgenic strain DA2123 (LGG-1::GFP) in which decrease in the GFP puncta represents a declined flux in the autophagosome formation [36]. We observed a significant decrease in the number of puncta (thus validating findings from qPCR experiments) after RNAi of PQC genes (Fig. 5A and supplementary table F).

Neurodegenerative diseases, including Parkinson's and Alzheimer's, are characterized by neuronal cell death. It has been observed that certain transcription factors can link major molecular machinery together like FOXO3 (which can interlink autophagy and apoptotic machinery). These act as surveillance systems in the cell to monitor perturbations in the autophagy process and finally negotiate apoptotic process when the clutter is not cleared by autophagy. We executed quantitative-PCR of the few previously reported apoptotic genes (*cep-1, ced-4, jnk-1, jkk-1* and *nsy-1*) after RNAi of PQC genes to investigate whether the knockdown of PQC genes which create an imbalance in the autophagic process, do have any impact in the cell death process by impacting apoptotic pathway [37–40]. *cep-1* encodes an ortholog of human tumor suppressor p53 that promotes DNA damage induced-apoptosis [41]. *jnk-1* encodes a serine/threonine kinase and its direct activator *jkk-1* are members of C-Jun N-terminal kinases (JNKs) involved in apoptotic signaling in both intrinsic and extrinsic pathways [42,43]. NSY-1, is the ortholog of the mammalian apoptosis signal-

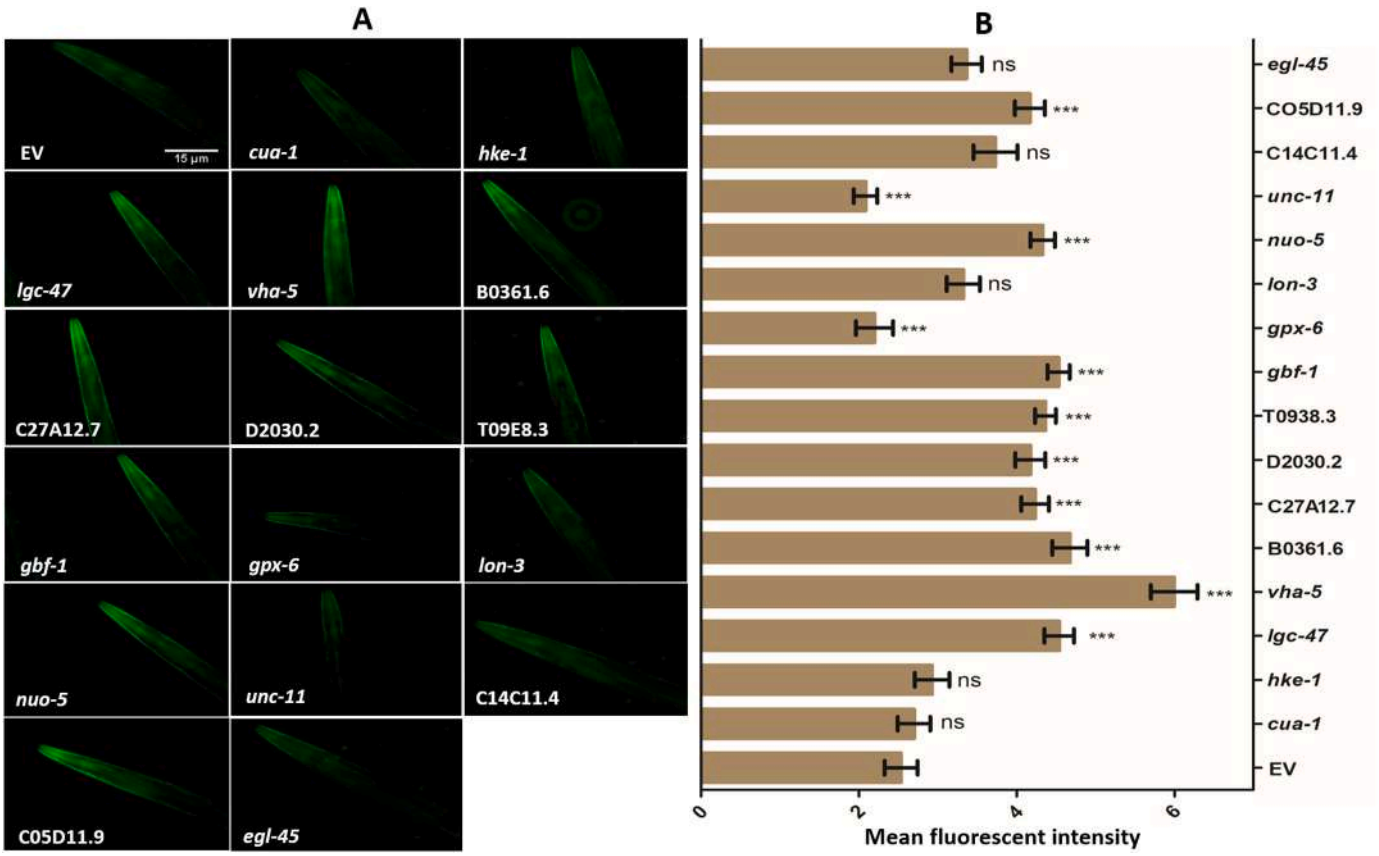

Fig. 2. Expression pattern of α-synuclein expression and accumulation in transgenic *C. elegans* strain NL5901 after knockdown of predicted downstream target genes of miR-4813-3p: (A); Shows α-synuclein accumulation in NL5901 after RNAi silencing *of cua-1, hke-4.1, lgc-47, vha-5,* B0361.6, C27A12.7, D2030.2, T09E8.3, *gbf-1, gpx-6, lon-3, nuo-5, unc-11,* C14C11.4, C05D11.9 *and egl-45* (B); Shows graphical representation of the fluorescence intensity as quantified by Image J analysis and non-parametric independent *t*-test (Mean ± SEM; $*p < 0.05$, $**p < 0.005$, $***p < 0.0005$ & ns: non-significant).

regulating kinase (ASK) family responsible for regulating the viability of animals in anoxia [39].

We observed that knockdown of PQC genes leads to downregulation of most of the apoptotic marker genes, as shown in Fig. 4B and supplementary table G and H. These observations show that knockdown of PQC genes downregulates both autophagy and apoptotic pathways, which might be the reason for augmented α-synuclein accrual and cellular stress.

2.6. Altered expressions of studied genes were observed in transgenic *C. elegans* strains having deletion mutation of autophagy and apoptotic markers

The experimental evidence gathered thus far shows that silencing of PQC genes modulates the expression of autophagy and apoptotic markers. To further explore the association of PQC genes with autophagy and apoptotic pathways, we checked their expression levels in transgenic *C. elegans* strains where autophagy and apoptotic pathways are compromised as they have deletion mutation of autophagy and apoptotic marker genes, VC8: *jnk-1* (deletion mutants), KU2: *jkk-1* (deletion mutants),VC172: *cep-1* (deletion mutants) and VC424: *bec-1* (deletion mutants). Interestingly, we observed the down regulation of the PQC genes in the deletion mutant background of *C. elegans* as shown in figure (Fig. 6A and B and supplementary table I). Under *jnk-1* and *bec-1* deletion background, we have observed a significant decrease in the mRNA fold change of six PQC genes. Under *jkk-1* deletion background, except for *gbf-1* we observed a significant decrease in the mRNA fold change of PQC genes. Under *cep-1* deletion background, except for *gbf-1, vha-5* and *cup-5* background, we observed a significant decrease in the mRNA fold change of other PQC genes. These observations in the deletion background of specific autophagy and apoptotic markers, reveal that there is a downregulation of most PQC genes indicating an interdependence between PQC genes and autophagy-apoptotic pathways.

2.7. PQC predicted targets of miR-4813-3p get modulated after inhibition of autophagy and proteasomal pathways

Our data suggests an interdependent co-expression pattern between PQC genes with autophagy and apoptotic pathways. As it is well known that there are two major proteolytic pathways by which proteins are degraded inside the cell, the autophagosome-lysosomal-pathway (ALP) and the ubiquitin-proteasomal-system (UPS), we went on to explore the impact of shutdown of these machineries on PQC gene expression pattern. For that, we have pharmacologically inhibited autophagy and proteasomal pathways, which is validated by the downregulation of autophagy markers (Fig. 4D) and proteasomal subunits (Fig. 4E) along with elevated α-synuclein expression levels (Fig. 4C). We observed that in case of autophagy inhibition, expression of PQC genes (barring C27A12.7) has been found to be significantly down-regulated, whereas after proteasomal inhibition (except for *cpd-2* and *acs-1)* other PQC genes have shown down-regulation (Fig. 4F and supplementary table. J & K). This observation reflects the involvement of PQC genes in the regulation of two major protein degrading machineries, autophagosome-lysosomal-pathway and ubiquitin-proteasomal-system, responsible for the clearance of unwanted aggregated proteins.

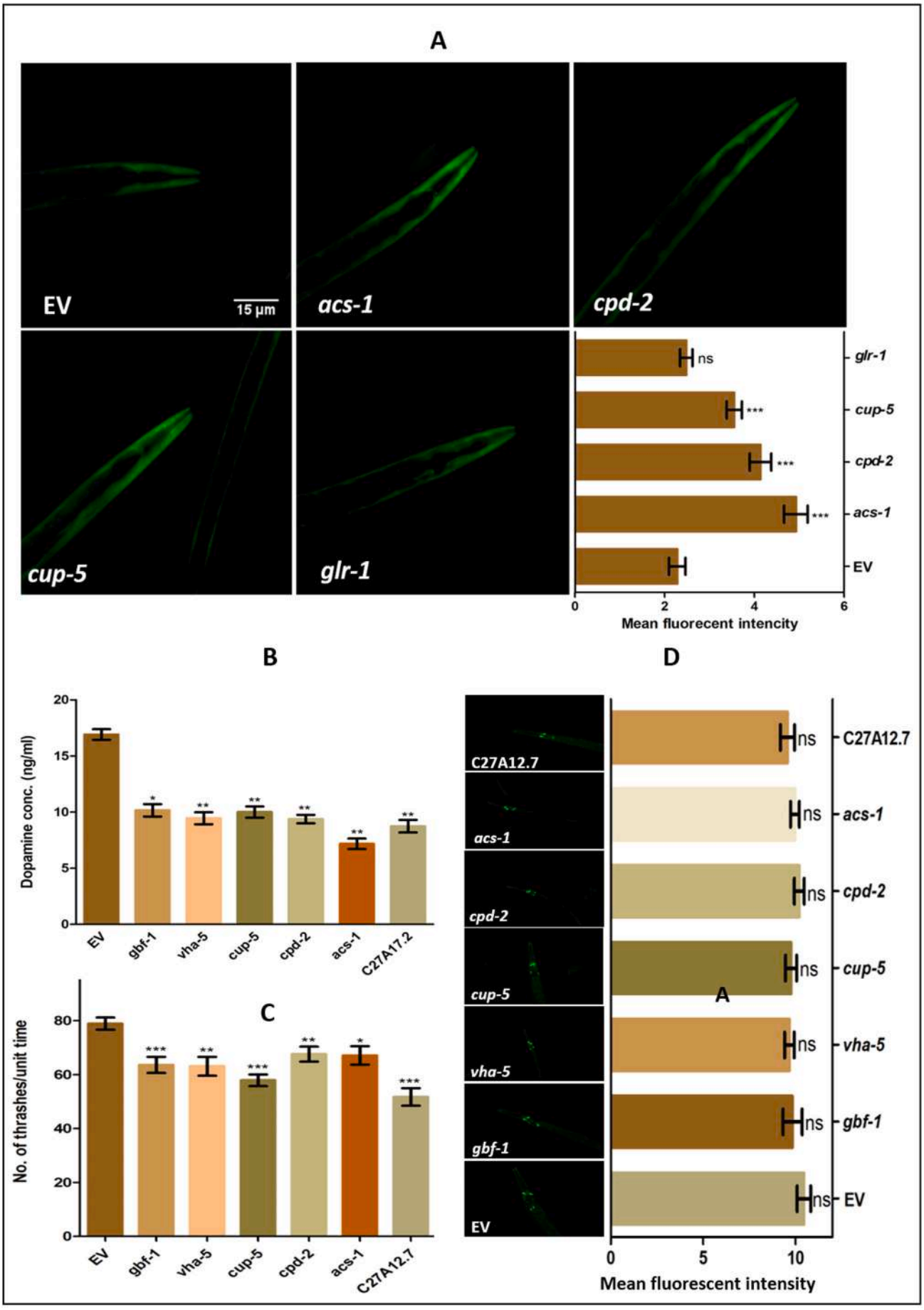

(caption on next page)

Fig. 3. Attenuated dopamine signaling and locomotory behavior is observed after knockdown predicted PQC targets of miR-4813-3p: (A); Shows α-synuclein accrual in NL5901 after RNAi silencing *acs-1, cpd-2, cup-5 & glr-1* post 75 h. The graphical representation shows the fluorescence intensity as quantified by Image J analysis and non-parametric independent t-test (*p < 0.05, **p < 0.005, ***p < 0.0005 & ns: non-significant) (B); Quantification of dopamine levels in transgenic *C. elegans* strain NL5901 after RNAi of PQC genes *(gbf-1, vha-5, cup-5, cpd-2, acs-1* & C27A12. 7). The graphical representation shows the fluorescence intensity as quantified by Image J analysis and non-parametric independent t-test (*p < 0.05, **p < 0.005, ***p < 0.0005 & ns: non-significant) (C); Quantification of the number of thrashes per unit time in transgenic *C. elegans* strain NL5901 after RNAi silencing of six PQC genes and (D); Expression pattern of DAT-1:: GFP in transgenic *C. elegans* strain BZ555 after RNAi silencing of six PQC genes. The fluorescence intensity was quantified by Image J analysis and non-parametric independent *t*-test are used to analyze the quantified fluorescent images, no. of thrashes and dopamine content (Mean ± SEM; *$p < 0.05$, **$p < 0.005$& ***$p < 0.0005$).

2.8. Elevated ROS levels and reduced longevity were observed after knockdown of PQC genes

Quality control (QC) pathways are aimed to identify and remove damaged proteins and organelles mainly by the autophagic pathway, which is crucial for post-mitotic cells such as neurons, to maintain homeostasis. Our experiments suggest that the silencing of PQC genes interferes in the autophagic pathway which could lead to oxidative stress due to accumulated defective mitochondrial proteins or by the damaged mitochondria [44–49]. To determine whether the putative PQC targets modulate ROS levels, we quantified the ROS levels under the knockdown condition of PQC targets in wild type worms. There was a significant increase in the fold change of ROS levels after knockdown of PQC genes (Fig. 5B and supplementary table L).

Reactive oxygen species can cause genotoxic and physiological damage when produced in excess amounts. Such accumulated oxidative stress leads to various cellular insults like DNA damage, modulating various signaling cascades, gene expression profile, peroxidation of lipids, and finally, protein homeostasis. Excessive oxidative stress can accelerate aging and could trigger neurodegeneration as well [46,50]. Therefore, we have performed the life span assay to check the effect on longevity after the silencing of PQC genes. Interestingly we observed a decrease in the life span of NL5901 strain after silencing of putative PQC downstream targets of miR-4813–3p. The median survival of NL5901 is 11, 10, 10, 10, 10 & 13 after knockdown of studied PQC genes, whereas the median survival of control was found to be 16 days (Fig. 5C).

2.9. Identification of possible pathways in which putative PQC downstream genes of miR-4813–3p are involved in causing neurodegenerative disease

After finding the strong association of predicted target genes of miR-4813–3p with quality control machinery mainly with autophagy and proteasomal clearance system, we further carried out studies towards identifying the possible pathways in which the identified PQC genes are involved as their down-regulation leads to the manifestation of PD pathological systems.

In the case of *gbf-1*, the literature suggests that *gbf-1* is involved in ER-Organization, endosomal transport, Mt-Organization and secretion [51–53]; therefore, we checked the expression levels of marker genes related to ER^{UPR} and MT^{UPR} systems. We found the results to be in concurrence with RNAi condition of *gbf-1* where we observed significant down regulation of most of the makers of both ER^{UPR} and MT^{UPR} pathways. In case of ER^{UPR}, we observed significant downregulation of *ire-1*, *hsp-6 and hsp-60*. In case of MT^{UPR}, we observed considerable downregulation of *hsp-6, hsp-60, clpp-1 and atfs-1* (Fig. 7A and supplementary table M).

vha-5 encodes a membrane-bound subunit of V0 domain associated with vacuolar proton translocating ATPase (V-ATPase) in the lysosome involved in regulating the acidic pH of lysosomal lumen; therefore, we checked the expression levels of lysosomal associated enzymes related to PD like *gana-1* and *gba-1* which are the human orthologues of α-galactosidase-A and β-glucosyl ceramidase, respectively [54–58]. We also checked the expression levels of marker genes (*hsp-1* and *imp-2*) associated with one of the lysosome-based autophagy pathways, i.e., chaperone-mediated autophagy (CMA) [59,60]. Significant down regulation of *hsp-1, imp-2*, *gana-1*, and *gba-1* was observed after RNAi of *vha-5* in NL5901 (Fig. 7B and supplementary table N).

The *cup-5* gene encodes an ortholog of the human mucolipin 1 gene; *cup-5* is required for viability, *endo*-lysosomal transport and the normal degradation of lysosomes [61–63]. Therefore, we checked the expression pattern of lysosomal enzymes associated with PD; *gba-1* and *catp-5*, *ctp-6* & *catp-7* which are the orthologues of human gene ATP_{13A2}. *This gene*, also known as *PARK9, responsible for the transport of polyamines in the cell, regulates lysosomal activity in cellular digestion and recycling. Mutation or lack of activity in ATP_{13A2} increases* genetic and environmental risk factors for Parkinson's [64,65]**.** We observed significant down-regulation of *gba-1, catp-5, ctp-6* & *catp-7* as a result of *cup-5* RNAi in NL5901 (Fig. 7C and supplementary table.O).

cpd-2 encodes a putative metallocarboxy peptidase orthologous to the human AEBP1 gene. We performed in silico studies and found genetic interaction between *cpd-2* and *imp-2* (supplementary fig. 2A), which is one of the markers of chaperone mediated autophagy; therefore, we further checked the expression levels of marker genes (*hsp-1* and *imp-2*) associated with CMA. We observed significant down regulation of all the marker genes *hsp-1* and *imp-2* as an effect of *cpd-2* RNAi in NL5901(Fig. 7D and supplementary table.P).

acs-1, an ortholog of human ACSF2 (acyl-CoA synthetase family member 2), is expressed in neurons and is involved in fatty acid metabolism [66,67]. With in silico studies we observed genetic correlations of *acs-1* with *daf-2* (via *itr-1*; *acs-1* is involved in IP3 signaling via *itr-1 receptor*) and with *bas-1* (supplementary fig. 2B and 2C) (which are involved in the biosynthesis of dopamine from tyrosine). We studied the expression levels of *itr-1*, *daf-16, cat-2*, and *bas-1* and found significant down regulations of these after RNAi of *acs-1* except for *daf-2* showing non-significant change in expression levels (Fig. 7E and supplementary table.Q).

C27A12.7 is an ortholog of human ARIH1 (Ariadne RBR E3 ubiquitin-protein ligase 1); we carried out in silico studies and found its correlation with *ubc-18* (which encodes for an E2 ubiquitin enzyme similar to human UBCH7), which has further associations with proteasome beta subunits (*pbs-1, pbs-3, pbs-4, pbs-6* & *pbs-7*) supplementary fig. 2D. We further investigated the expression levels of these genes after RNAi of C27A12.7 in NL5901 and observed that these are significantly downregulated (Fig. 7F and supplementary table R). The reported functional aspect of these studied genes, is summarised in supplementary table S.

Table 2
miR-4813-3p via its predicted downstream targets modulates α-synuclein accrual in transgenic *C. elegans*:

Downstream targets of miR-4813-3p	Pathway Involved
acs-1	Protein Quality control
vha-5	
C27A12.7	
cpd-2	
gbf-1	
cup-5	
nuo-5	Mitochondrial bioenergetics
C05D11.9	
D2030.2	
lgc-47	Ion channel
T09E8.3	Synaptic transmission
B0361.6	Predicted to have methyltransferase activity

*Source: Worm base version: WS275.

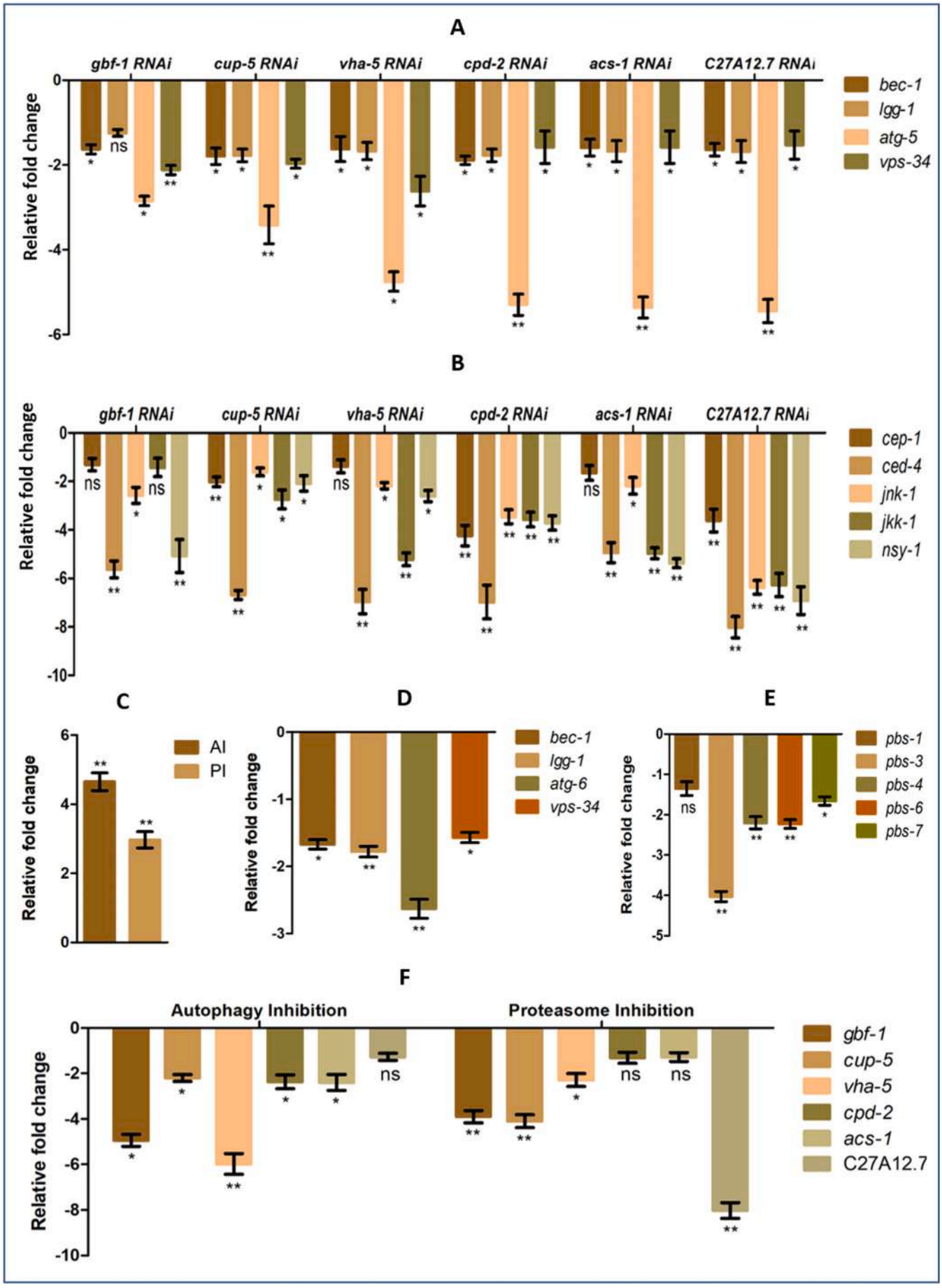

(caption on next page)

Fig. 4. Modulation of autophagy, apoptotic and PQC genes in NL5901 strain:(A); Quantitative PCR patterns of autophagy markers *bec-1, lgg-1, atg-5 & vps-34* (B); Quantitative PCR patterns of apoptotic markers *cep-1, ced-4, jnk-1, jkk-1* and *nsy-1* in transgenic *C. elegans* strain NL5901 after RNAi silencing of predicted PQC downstream genes *gbf-1, vha-5, cup-5, cpd-2, acs-1* & C27A12.7. (C); Quantitative PCR patterns of α-synuclein expression levels in transgenic *C. elegans* strain NL5901 after pharmacological inhibition of Proteasome and Autophagy (D); Quantitative PCR patterns of autophagy markers *bec-1, lgg-1, atg-5 & vps-34* (E); Quantitative PCR patterns of proteasome subunits *pbs-1, pbs-3, pbs-4, pbs-6&pbs-7,* (F); Quantitative PCR patterns of PQC genes (*gbf-1, vha-5, cup-5, cpd-2, acs-1* & C27A12.7) in transgenic *C. elegans* strain NL5901 after inhibition of Autophagy machinery, quantitative PCR patterns of PQC genes (*gbf-1, vha-5, cup-5, cpd-2, acs-1* & C27A12.7) in transgenic *C. elegans* strain NL5901 after inhibition of Proteasome machinery. Fold change are quantified using non-parametric independent *t*-test (Mean ± SEM; $*p < 0.05$, $**p < 0.005$, $***p < 0.0005$ & ns: non-significant). Actin (*act-1*) is used as an endogenous control with which ct values of each gene is normalized. AI: Autophagy Inhibition and PI: Proteasomal Inhibition.

3. Discussion

The build-up of aberrant and malformed proteins is known to be the key cause of effects linked with age-associated neurodegenerative diseases. In a healthy state, the clearance of such noxious accumulations is maintained via an efficient protein clearance system involving the autophagic–lysosomal network, ubiquitin-proteasome system or by chaperone mediated autophagy [68]. Considering the multiple factors that govern various checkpoints of these pathways, we endeavored to identify a common trigger behind these phenomena. Since single miRNA molecules are known to regulate multiple genes [69], we carried out miRNA profiling and identified miR-4813-3p that was significantly downregulated in *C. elegans* strain expressing human α-synuclein. Interestingly, we observed strong functional association of this miRNA molecule despite its low abundance. This phenomenon has also been previously observed in context of colon tumor wherein low abundance miR-206 was reported to regulate cell fate [70]. Our studies further led to the identification of six predicted downstream targets of miR-4813-3p namely *gbf-1, vha-5, cup-5, cpd-2, acs-1* and C27A12.7, which are directly related to the protein quality control system.

3.1. Modulation of α-syn accumulation by PQC genes

Elevated levels of α-syn as a result of its accumulation within tissues are well documented in PD [71,72]. This fact prompted us to study the effect of PQC gene silencing in association with α-syn accrual. We observed a significant increase in the α-syn accrual after silencing of identified PQC genes. *gbf-1* is reported to be involved in the endoplasmic reticulum and mitochondrial organization. We observed that knockdown of *gbf-1* significantly downregulates ER^{UPR} and MT^{UPR} markers. Such a compromised UPR pathway may be the possible reason for α-synuclein accumulation [73,74]. Lysosomal associated autophagy is the main pathway for the clearance of highly unfolded and aggregated proteins inside the cell. Compromising the lysosomal pH by knockdown of *vha-5* (lysosomal V-ATPases) will not only alter the proper functioning of lysosomal hydrolytic enzymes but also, we observed downregulation of associated lysosomal enzymes related to PD [75–77]. These findings suggest that *vha-5* is necessary for the clearance of aggregated α-syn. *cup-5* is being reported to be involved in normal lysosomal viability, degradation and calcium ion homeostasis. Our experimental results also complement the above findings as knockdown of *cup-5* has downregulated not only lysosomal associated enzymes related to PD but also a lysosomal P-type ATPase that has involvement in

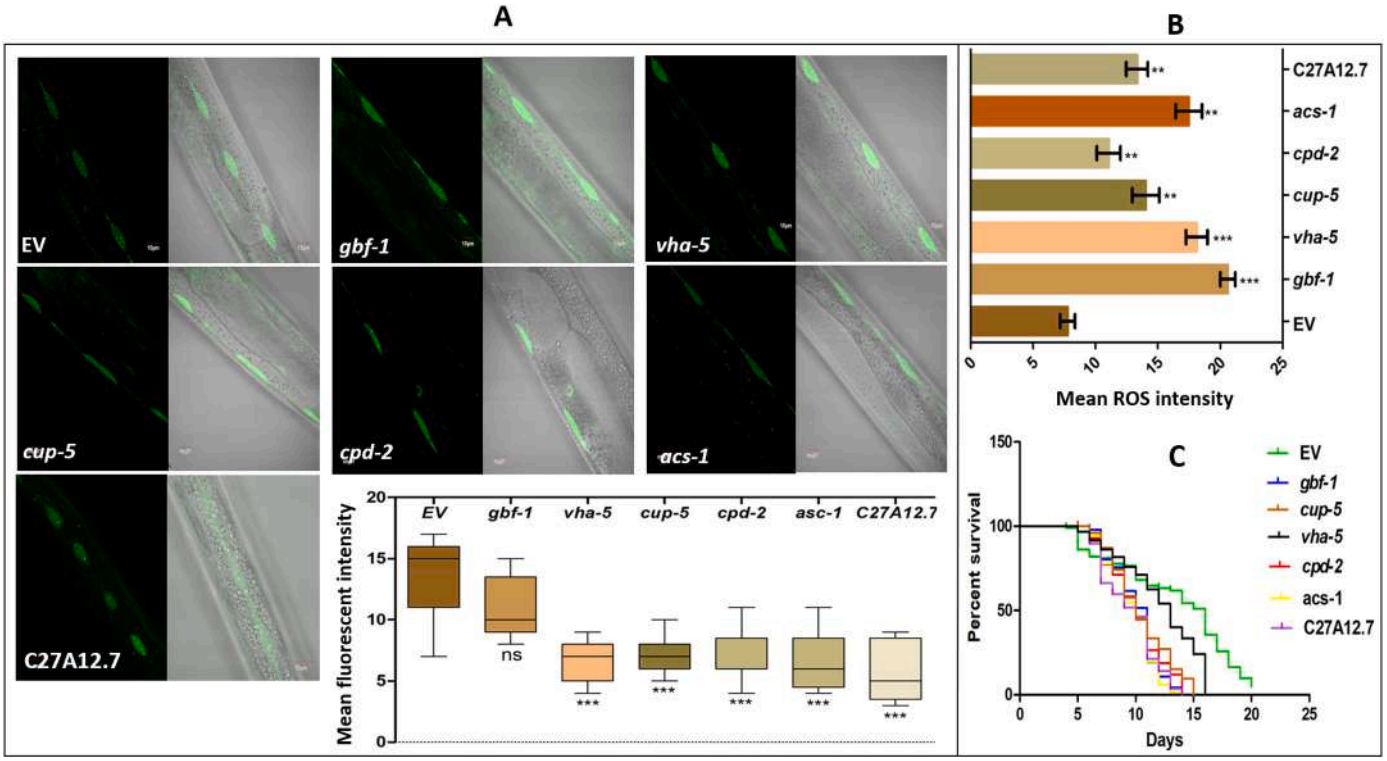

Fig. 5. Modulation of major PD associated endpoints (LGG-1, ROS & longevity) after RNAi of PQC genes (*gbf-1, vha-5, cup-5, cpd-2, acs-1* & *C27A12. 7*): (A); Expression pattern of LGG-1: GFP in transgenic *C. elegans* strain after RNAi silencing of six PQC genes in DA2123 strain. (B); Quantification of ROS in wild-type *C. elegans* strain N2 after RNAi knockdown of six PQC genes. (C); Survival curve of NL5901 after RNAi silencing of PQC genes. The fluorescence dots were quantified by Image J analysis and a non-parametric independent t-test was used to analyzed quantified fluorescent images and ROS values (Mean ± SEM; $*p < 0.05$, $**p < 0.005$& $***p < 0.0005$). For life span, Data was analyzed by Kaplan Meier survival curve.

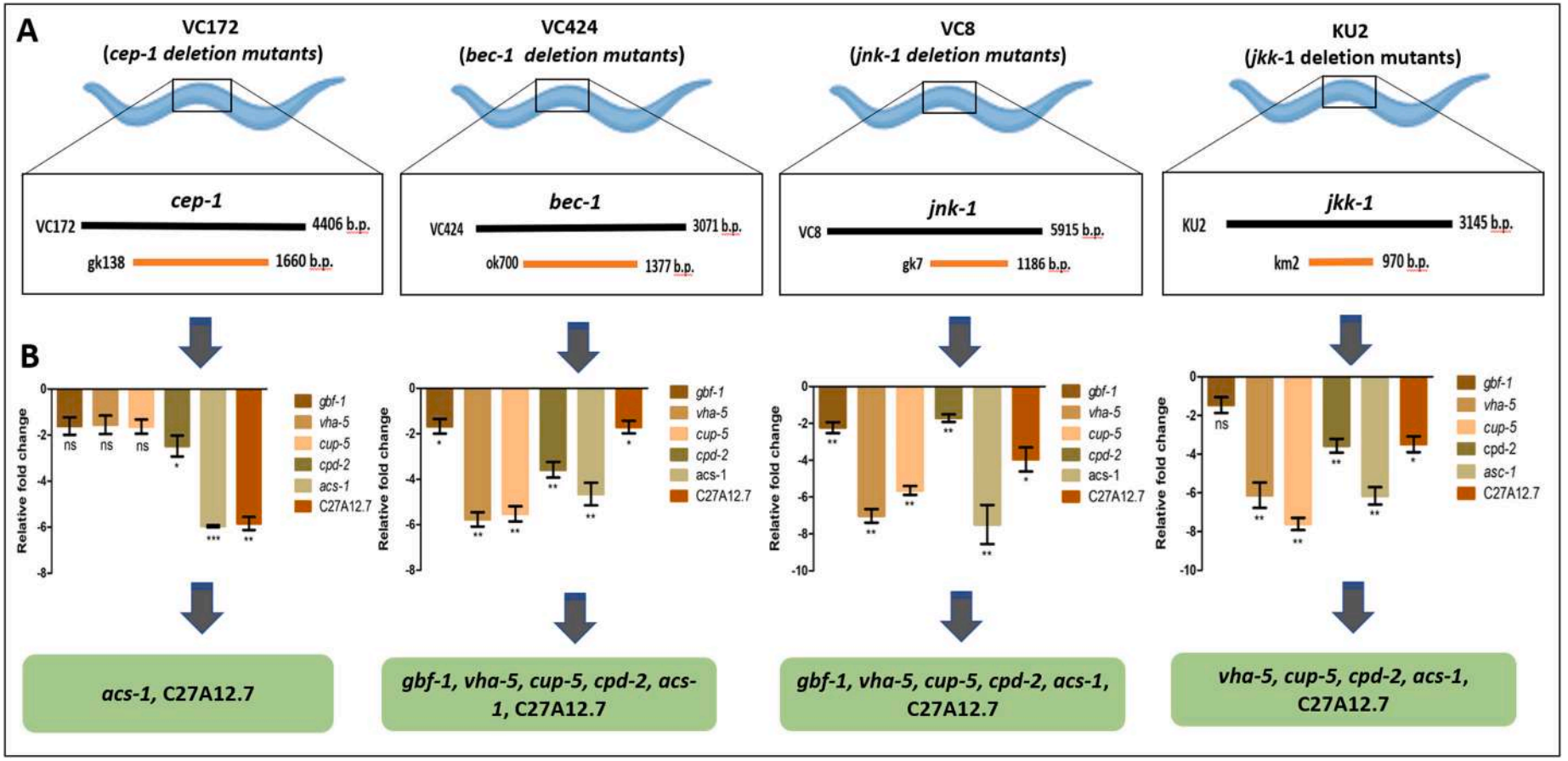

Fig. 6. Modulation of PQC genes under deletion background of autophagy and apoptotic deletion mutants: (A); Transgenic *C. elegans* strains having deletion mutation of autophagy and apoptotic makers, VC172: *cep-1* (deletion mutants), VC424: *bec-1*(deletion mutants), VC8: *jnk-1*(deletion mutants) and KU2: *jkk-1* (deletion mutants), (B); Quantitative PCR expression patterns of PQC genes (*gbf-1, vha-5, cup-5, cpd-2, acs-1 & C27A12.7*) in transgenic *C. elegans* strain VC8, KU2, VC172 & VC424. Fold change are quantified using and non-parametric independent *t*-test (Mean ± SEM; $*p < 0.05$, $**p < 0.005$, $***p < 0.0005$ & ns: non-significant). Actin (*act-1*) is used as an endogenous control with which ct values of each gene is normalized.

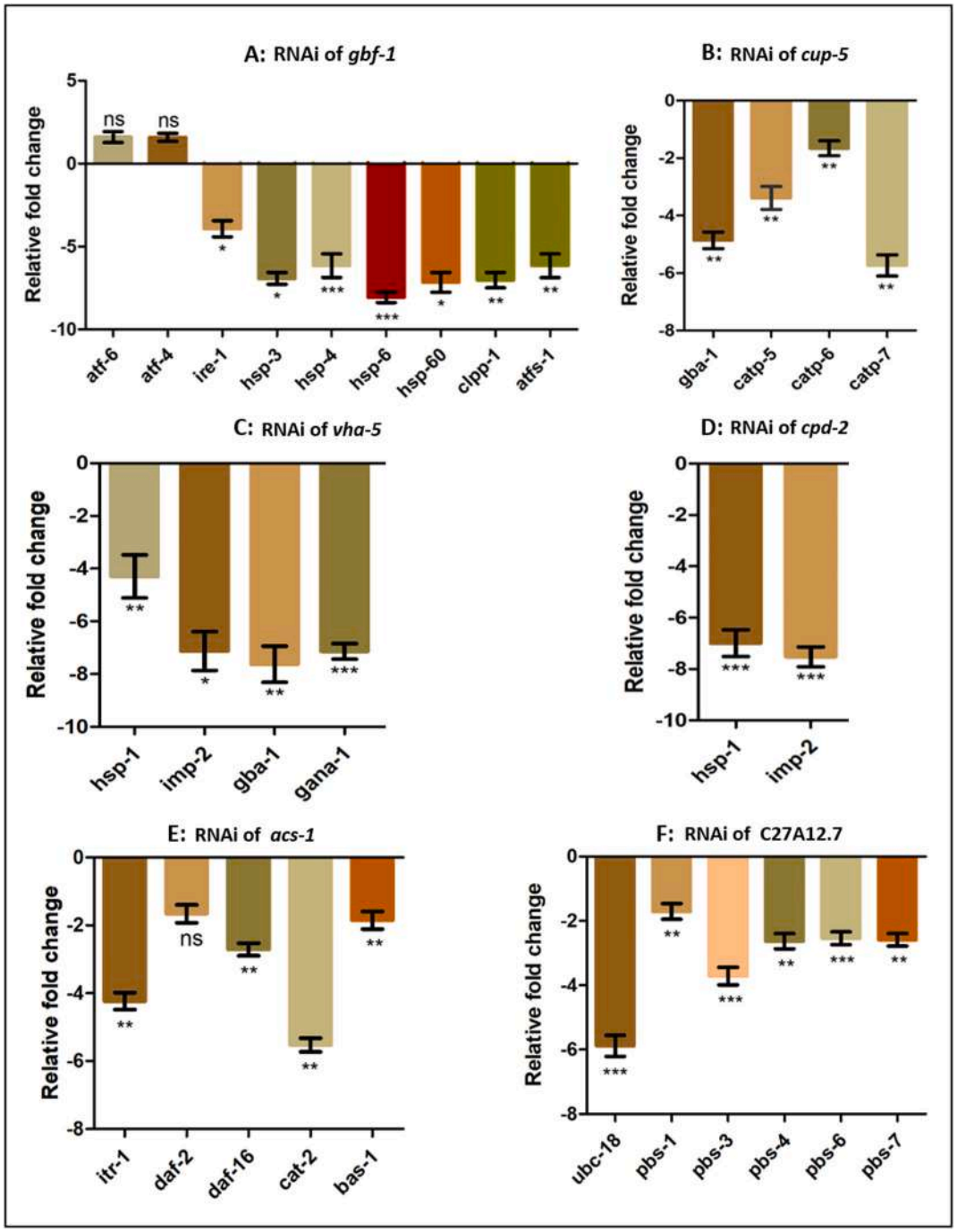

Fig. 7. Modulation of major marker genes of various pathways after RNAi of PQC genes (*gbf-1, vha-5, cup-5, cpd-2, acs-1&C27A12.7*): (A); Quantitative PCR patterns of ER^{UPR} marker genes (*atf-6, atf-4, ire-1, hsp-3, hsp-4 and hsp-4*) and MT^{UPR} marker genes (*hsp-6, hsp-60, clpp-1* and *atfs-1*) after silencing of *gbf-1* gene (B); qPCR expression patterns of *catp-5, ctp-6 &catp-7* and lysosomal associated enzymes *gba-1* after silencing of *cup-5* gene (C); qPCR expression patterns of chaperone mediated autophagy marker genes (*hsp-1 & imp-2*) along with lysosomal associated enzymes like *gaba-1* and *gba-1* related to PD after silencing of *vha-5* gene (D); qPCR time expression patterns of chaperone mediated autophagy marker genes (*hsp-1 & imp-2*) after silencing of *cpd-2* gene (E); qPCR expression patterns of *itr-1, daf-2*, *daf-16, cat-2* and *bas-1* after silencing of *acs-1* gene (F); qPCR expression patterns of *ubc-18*& proteasomal beta subunits *ubc-18, pbs-1, pbs-3, pbs-4, pbs-6&pbs-7*after silencing of *acs-1* gene. All the above mRNA expression levels were observed in transgenic *C. elegans* strain NL5901. Quantified by and non-parametric independent t-test (Mean ± SEM; *p < 0.05, **p < 0.005). Actin (*act-1*) is used as an endogenous control with which ct values of each gene is normalized.

calcium ion homeostasis. Therefore, altering the normal turnover of lysosomes with unregulated Ca^{+2} homeostasis could be the possible reason for elevated α-syn accrual [78,79]. *cpd-2* is a metallo carboxy peptidase; we observed in the in silico studies that *cpd-2* has genetic interactions with markers of chaperone-mediated autophagy (CMA) and RNAi of *cpd-2* led to downregulation of the markers of CMA (*hsp-1* and *imp-2*) which is one of the dedicated events responsible for the partial clearance of redundant soluble cytoplasmic proteins in PD [80,81]. Our findings also substantiate with one of the studies where *imp-2* inhibition leads to compromised proteasomal activity and chaperone-mediated autophagy clearance pathway in context of glucotoxicity in *C. elegans* [82] .This could be one of the possible reasons for the upsurge in α-syn accrual after the silencing of *cpd-2*. RNAi of *acs-1,* which is expressed neuronally and is involved in fatty acid metabolism, down-regulated

daf-16 transcription factor and the enzymes involved in dopamine synthesis from tyrosine (based on the clues from in silico genetic interaction). Existing literature shows that loss of *daf-16* and reduced dopamine levels are one of the major factors in PD ailments by augmenting the α-syn aggregation [28,83]. Possibly this could be a reason for increased α-syn accrual after silencing of *acs-1*. Based on existing literature, C27A12.7 is predicted to have ubiquitin-protein transferase activity, and we have validated the down-regulation of proteasome beta subunits after silencing of C27A12.7. Earlier reports suggest reduced proteasomal activity in substantia nigra of PD patients [84–86]. Therefore, it is likely that the silencing of C27A12.7 can lead to α-syn accrual associated with proteasome dysfunction.

3.2. Involvement of PQC genes in redox homeostasis

Oxidative stress is an essential factor that is associated with PD, along with α-syn [87–89]. Therefore, we studied the ROS levels after the silencing of identified PQC genes, and interestingly we observed elevated ROS levels after knockdown of each of the identified genes. Apart from vesicular transport *gbf-1* (GTPase ARF) is involved in mitochondrial homeostasis. Such a similar pattern of defects was also observed in mammalian and yeast cells [53]. Therefore, knockdown of *gbf-1* leads to impaired mitochondrial functioning manifesting elevated ROS levels inside the cell. *vha-5* is a component of lysosomal V-ATPases. It is reported that disturbance in the lysosomal functional composition leads to a decrease in the cardiolipin content (as a cross-talk signaling between lysosome and mitochondria), which leads to mitochondrial fission accompanied by deregulation in mitochondrial function and ROS generation [90]. This substantiates the observation of elevated ROS production after the silencing of *vha-5*. *cup-5* is an ortholog of human mucolopin1 (MCOLN1), also known as TRPML1, a vital calcium ion channel on the membrane of the lysosome. Activation of TRPML1 is well reported to maintain the homeostasis inside the cell by maintaining the clearance of damaged mitochondria and excess ROS by activating the autophagy process; therefore, knockdown of *cup-5* has shown elevated ROS within the cells [91]. Silencing of *cpd-2*, an ortholog of human carboxypeptidase (CPM), led to elevated ROS levels; previously, it has been reported that upregulation of protective genes including CPM, led to antioxidant effects in a patient who was at the risk of developing anemia thus substantiating the observed correlation [92]. From in silico studies, we found genetic correlations of *acs-1* with *itr-1* (*acs-1* has been reported for the optimal IP3 signaling, and *itr-1* encodes for inositol 1,4,5-trisphosphate receptor (IP3R)). Recent studies have shown that cell lines devoid of IP3R (DT40 cell lines) have higher ROS levels with downregulated glutathione and superoxide dismutase 2 (SOD2) as compared to wild type. This supports our evidence of elevated ROS levels after the silencing of *asc-1* in NL5901 [93]. C27A12.7 is an ortholog of human ARIH1 (Ariadne RBR E3 ubiquitin-protein ligase 1). ARIH1 polyubiquitinates damaged mitochondria and direct them for degradation by autophagy [94]. Therefore, after knocking down of C27A12.7 we observed elevated ROS levels probably because its knockdown perturbs the damaged mitochondrial removal in the cell.

3.3. Amelioration of dopamine levels and locomotory behaviour

Impairment of specific neuronal populations inside the brain is one of the features of PD. The dopaminergic neurons of substantia nigra pars compacta are the most susceptible ones as the disease progresses [95]. Therefore, we investigated the dopamine levels after the silencing of identified PQC genes, and strikingly we observed downregulated dopamine levels after knockdown of each PQC gene. *gbf-1* is predicted to have ARF guanyl-nucleotide exchange factor activity; existing literature supports the fact that ARF-GTPase like gene products alleviate neurodegeneration by improving the protein trafficking towards lysosome. Other findings suggest that ARF guanyl-nucleotide exchange factor activity interacts with neuronal calcium sensor-1 in the calcium signaling pathway, determining the *C. elegans* locomotion at elevated temperature [96,97]. Therefore, it seems likely that the silencing of *gbf-1* is not neuroprotective for dopaminergic neurons. Lysosomal acidification is necessary for the proper functioning of hydrolyzing enzymes in it. One of the findings suggests that compromising lysosomal acidification by tumor necrosis factor-α can lead to the accumulation of α-syn in the dopaminergic neurons leading to cell death [90]. Impaired lysosomal acidification by knockdown of *vha-5* in present studies, could be the possible cause of dopaminergic neuronal damage. It is well reported that Ca^{+2} homeostasis disruption in neuronal cells can lead to impaired neuronal functions, which progressively can lead to neurodegenerative diseases such as PD. Dopaminergic neuronal death has been reported either by knockdown of TRPC1 (transient receptor potential (TRP) channel superfamily, which includes mucolipin) or the addition of TRPC channel blockers. Therefore, knockdown of *cup-5* (orthologue of human mucolipin) may be involved in dopaminergic neurodegeneration by disrupting the Ca^{+2} homeostasis inside the neuron [98]. Carboxy Peptidase E (CPE) plays an important role in the nervous system. It is required for proper neuronal structure (dendrite patterning), neuronal survival (hippocampal neurons) & proper cognitive function. *cpd-2*, an ortholog of human CPM, shares around 65 % homology with CPE. Therefore, possibly the role that CPE is playing in the hippocampal neurons, *cpd-2* might play for the dopaminergic neurons in the substantia nigra, though further investigation is required for analyzing such specific role [99]. In recent studies, overexpression of mutated α-synuclein has been shown to lead to the accumulation of triacyl glycerol (TAG) in dopaminergic neurons. Elevated neuronal TAG content was associated with increased activity of the Acyl-CoA synthetase [100,101]. *acs-1* is a human orthologue of acyl-CoA synthetase family member 2; therefore, knockdown of *acs-1* is probably hampering the lipid metabolism inside the dopaminergic neurons making these further vulnerable. C27A12.7 is an ortholog of human E3 ubiquitin-protein ligase 1. It has been reported that endogenous PARKIN plays an essential role in dopaminergic neuronal protection from mitochondrial stress [102]. Therefore, the silencing of C27A12.7 makes dopaminergic neurons more susceptible to elevated mitochondrial stress. In PD the dopamine transporter (DAT-1) can be a critical factor for maintaining of the dopamine concentration [26]. But after knockdown of identified putative PQC downstream targets, we observed that there is a non-significant variation in DAT-1 expression levels even though we observed significantly reduced levels of dopamine. It is known that locomotory deficits in case of PD are associated with decline in dopamine levels, [103,104] hence the observed effect on locomotory behavior, vis studying thrashing of worms, could be because of reduced neurotransmitter dopamine levels following silencing of predicted PQC downstream targets.

Autophagy is a highly conserved evolutionary cellular process that plays a crucial role not only in maintaining the cellular homeostasis (by degrading misfolded proteins and damaged organelles) during stress situations but also takes part in remodeling during the developmental process [28,105]. As neurons are the most long-lived post-mitotic cells, brain becomes one of the most vulnerable organs for the mutations involved in autophagic pathways and lysosomal disorders, which leads to the pathobiological feature of many neurodegenerative disorders. We observed that the silencing of identified PQC genes down-regulates the autophagy markers (*bec-1, lgg-1, atg-5* and *vps-34*) significantly. BEC-1 plays an essential role in the functioning of class III PI3 kinase; it is an important protein required for autophagy, endocytosis, and membrane trafficking [33]. On the other hand, interestingly, we have observed down-regulation of PQC genes in the *bec-1* deletion mutant background of *C. elegans*, which indicates a strong association between *bec-1* and PQC gene expressions. *vps-34* encodes an ortholog of the phosphoinositide 3-kinase and is required for vesicular trafficking, including autophagy and apoptotic cell clearance. *lgg-1* encodes the ortholog of mammalian MAP-LC3 required for the degradation of cellular components [34,35]. We further validated LGG-1 expression levels with a

decrease in the GFP puncta, which imitates curtailment in the autophagosome formation in DA2123 transgenic strain of *C. elegans* after silencing of PQC genes. Even after impeding the autophagy and proteasome machinery pharmacologically, we observed downregulation of most of the PQC genes, which shows a substantial alliance of PQC genes with the protein clearance system.

3.4. Alteration of autophagy and apoptotic process

Among diverse cell death pathways involved in PD pathogenesis, apoptosis plays a critical role. It is not only necessary for building a decisive neuronal network in the developing brain but also plays an important role in eradicating the damaged neurons as the aging progresses. Although excessive, uncontrolled apoptosis has been reported to accelerate the disease progression in PD [106], we observed that silencing of identified PQC genes down-regulates the apoptotic markers (*cep-1, ced-4, jnk-1, jkk-1* and *nsy-4*) significantly. *cep-1* encodes an ortholog of human tumor suppressor p53 that promotes DNA damage induced-apoptosis. Programmed cell death is initiated by *ced-4*, which activates *ced-3* and in turn encodes the caspase required for the execution of apoptosis [41]. *jnk-1* encodes a serine/threonine kinase and its direct activator, *jkk-1* are members of C-Jun N-terminal kinases (JNKs), which belongs to the MAP-kinase superfamily. Both are expressed in most of the neurons and mediate apoptotic signaling in both intrinsic and extrinsic pathways [42,43]. NSY-1, is the ortholog of mammalian apoptosis signal-regulating kinase (ASK) family of MAP kinase (MAPK) kinase kinases (MAP3Ks) responsible for regulating the viability of animals in anoxia [39]. We also observed that most of the PQC genes were down-regulated *under cep-1, jnk-1 & jkk-1* deletion mutant background, which shows a relevant involvement of PQC genes with the apoptosis process. Both autophagy and apoptosis protect the cell or the nearby cell during an adverse situation. Therefore, a balance between apoptosis and autophagy becomes crucial to maintain normal physiological function. Downregulation of apoptotic and autophagy markers under the knockdown condition of PQC genes and vice versa suggests their core involvement in both of the QC process. Though we have provided some probable mechanistic insight of PQC gene involvement in certain pathways (that can directly or indirectly affect the overall quality control network), still to get a clear picture of their regulatory role in autophagy and apoptosis needs further investigation.

Based on our experimental results we can say that we have identified six PQC genes (*gbf-1, vha-5, cup-5, cpd-2, acs-1 & C27A12. 7*) playing a vital role in PQC machinery therefore any mimetics or drugs that can over express the human orthologue (GBF-1, ATP6V0A 1/2, MCOLN 1/3, CPE/ CPN1, ACSF2 and ARIH1 respectively) of these six genes could possibly play a potential therapeutic target for drug development for the Parkinson's patients. The future implications of the present study would be regarding understanding the mechanistic aspects and regulation of PQC genes via miR-4813-3p, particularly in the context of aging, which could be achieved with efficiency via employing the various developmental stages of *C. elegans*.

4. Conclusion

Neurodegenrative PD exhibits impairment in clearance of toxic protein aggregates, which ultimately leads to neuronal cell death, decline in essential neurotransmitter levels and declined bodily functions. Employing transgenic *C. elegans* strain that expresses 'human' alpha synuclein, we report on the the novel role of micro RNA molecule miR-4813-3p in regulating the various pathways associated with proteostasis network via its predicted downstream targets (*gbf-1, vha-5, cup-5, cpd-2, acs-1* and C27A12.7). Our studies show that the absence of putative downstream targets of miR-4813-3p clutter the PQC network via α-syn accrual and its associated outcomes which further impact autophagy and apoptotic pathways. The studies propose miR-4813-3p as a common trigger for multiple factors associated with PD. The findings are a step towards exploring potential of this, and other, micro RNA molecules towards pharmacological manipulations in the interest of bettering mechanistic understanding to Parkinson's disease.

5. Methods

5.1. C. elegans culture and maintenance

For our studies, we have used an *Escherichia coli* stain (OP50) to deliver as a source of food. OP50 seeding was done to prepare bacterial lawn onto NGM plates. Nematode Growth Medium was prepared by adding 2.5 g Peptone (sigma),3 g NaCl (sigma),17 g agar (HIMEDIA). After the solution is autoclaved around 50 °C,1 ml cholesterol (5 mg/ml), 1 ml $MgSO_4$(1 M), 1 ml $CaCl_2$(1 M), 25 ml KH_2PO4(1 M pH 6.0) was added. Then the media was poured on 90 mm petri plates under sterile conditions and left till it solidify. After sterilizing the plates by U.V. treatment, plates are stored at 4 °C. The bacterial lawn was prepared by spreading 500 μl of OP50 on NGM plates with the help of a spreader under sterile conditions, which were incubated overnight at 22 °C. Subculturing of *C. elegans* strains were performed on these pre-seeded OP50-NGM plates and propagated further at 22 °C.

5.2. C. elegans embryo isolation

From previously chunked *C. elegans* grown on OP50 seeded NGM plates, gravid reproductively mature *C. elegans* population was harvested by using M9 buffer. Worms were settled down in a 15 ml conical centrifuge tube by centrifugation at 1300 rpm for 2 mins. Settled worms were resuspended in M9 buffer and washed thrice in order to remove any adhering bacteria on the surface of worms. Finally, to the worm pellet, 2 ml of sodium hypochlorite and 1 M sodium hydroxide solution hypochlorite (the axenizing solution) was added. To dissolve the worm body, the whole solution was gently mixed to release the embryos. The derived embryos were pelleted down via centrifugation for 5 mins at 1300 rpm. The pelleted embryos were then washed with M9 buffer thrice and was spread onto experimental treatment plates under sterile conditions.

5.3. C. elegans strains

Strains used in this study were N2; Bristol wild-type, NL5901; pkIs2386 [unc-54p::alpha-synuclein::YFP + unc-119(+)] [106](**97**), DA2123; adIs2122 [lgg-1p::GFPC rol-6(su1006)] and BZ555; egIs1 [dat-1p::GFP]. From *Caenorhabditis* Genetics Center (University of Minnesota, Minneapolis, MN) entire strains were received. All the strains are propagated at 22 °C either on OP50 or on RNAi treatment plates.

5.4. RNAi-induced gene silencing

RNAi-Induced feeding protocol was used for the silencing of specific genes. Bacterial clone expressing dsRNA (source Ahringer library) targeted for *C. elegans* was first cultured for 6–8 h in Luria Bertani Broth media containing ampicillin (50 μg/ml). When the culture attains its active log phase,500 μl of this bacterial culture was seeded onto NGM plates (having 5 mM IPTG and carbenicillin; 25 mg/L) incubated overnight at 22 °C. Under sterile conditions, embryos of the desired strain were transferred to these treatment plates.

5.5. Image acquisition

Synchronized worms were washed thrice with M9 buffer to remove adhering bacteria from the treatment plates and immobilized with 100 mM sodium azide (Sigma, Cat No. 71289). Immobilized worms were mounted on a clean glass slide with the help of a coverslip. Finally, the images of the worms were captured using Carl Zeiss Axio ImagerM3 for α-synuclein protein expression/accumulation experiment and a

multiphoton confocal microscope to capture the images of transgenic *C. elegans* strains NL5901 and DA2123, respectively. ZEN2010 image acquiring software was used for image acquisition, and images are finally quantified through Image J software (Image J, National Institutes of Health, Bethesda, MD).

5.6. Estimation of Reactive Oxygen Species (ROS)

ROS estimation was done by using 2,7-dichlorodihydrofluorescein diacetate (H_2DCFDA). Both control and RNAi silenced groups of worms were washed three times with M9 buffer and two times with phosphate buffer saline (PBS). Each group (of around 100 worms/100 ml assay solution) was analyzed in triplicates and finally transferred to assay wells (OptiPlate-96 F; PerkinElmer). 100 μl H_2DCFDA (Cat. No. D399, Invitrogen) from 100 mM stock prepared in ethanol was added to each well. Quantification of the fluorescence intensity from each well was taken at three discrete time intervals, (i); before the dye was added (ii); instantly after the addition of dye and (iii); 1-hour post-incubation after the dye was added. Multimode plate reader (Perkin Elmer, VICTOR X3) was used to measure the fluorescence intensity having an excitation wavelength of 485 nm and an emission wavelength of 520 nm. The difference in the fluorescence was determined by subtracting the initial reading (before the addition of dye) from the readings of the immediate addition of dye, which was finally subtracted from the reading of post 1 h incubation of dye. Finally, fluorescence intensity per worm was plotted as its mean value. Statistical significance was evaluated as by student's *t*-test using GraphPad Prism software. For ROS estimation in N2 strain, we have performed the experiment in three replicates and in each experiment, we have taken 100 worms for each group.

5.7. Estimation of neurotransmitter dopamine levels using LC-MS/MS

Using LC-MS/MS, dopamine content of both control and treatment worms were measured. Age synchronized adult worms (L4 stage) were washed thrice with M9 buffer to remove adhering bacteria on it. Worm pellet was flash frozen using liquid nitrogen. The lysis of worms is carried out by using the sonicator (at 30 % amplitude for 5 min (pulse rate 2 s on/off) using 300 μl Tris buffer (pH = 8). Lysate samples were centrifuged for 10 min at 13000 rpm in 4 °C, and the supernatant was collected (the extracted protein sample) which is quantified by the Bradford method. The LC consists of Delta 600 binary pump WATERS (Manchester, UK) linked with 2707 autosampler and in-line AF degasser equipped with API 3200 triple, quadruple mass spectrometer (ABI SCIEX, ON, Canada). Using a basic protein precipitation technique, using acetonitrile (1:3) samples were processed; centrifuged for 20 min at 14,000 rpm and supernatant (20 μl) was injected into LC-MS/MS. The separation was accomplished using 150 × 4.6 mm, 2.6 μm Thermo Fischer scientific Accucore AQ column having an acetonitrile's mobile phase (with a 0.1 % formic acid (35:65) having a flow rate of 0.6 ml/min. For the sample, the total run time was 4.00 min. The ionization of dopamine was achieved in MRM positive mode with the transition of 154.00/137.2. Integration of Analytical data was performed by Analyst software version 1.6 (AB SCIEX, ON, Canada). For each group, 7000 worms were taken for estimation and dopamine concentration was achieved in ng/ml.

5.8. Assay for motility of worms

Worms motility is estimated by thrashing assay where the number of thrashes is counted in per unit time. One thrash means; one-way complete bending of the body to the extreme angle and return to the initial position. In our study, worms harvested from the treatment plates were washed three times with M9 buffer to remove the bacteria's adhering bacteria. On a drop of M9 buffer, a single worm was placed and the total number of thrashes in 30 s was counted using a timer under Sterio zoom microscope (Leica). Ten worms were counted for each group in a separate experiment (in duplicate). For each group randomly, ten worms were selected for thrashing count.

5.9. Total RNA isolation and cDNA synthesis

Age synchronized worms were washed thrice with M9 buffer and then twice with diethylpyrocarbonate (DEPC; Sigma Cat. No. D5758) treated water to discard adhering bacteria. To isolate the total RNA from all the different strains of *C. elegans* used in our study, we have used RNAzol® RT (Sigma, Cat. No. R4533) method as per the manufacturer's protocol. The RNA concentration was determined by using the UV spectrophotometer Nanodrop (Quawell-UV–Visible Spectrophotometer, Thermo-Q5000). One ng of total isolated RNA was used for preparing cDNA by using cDNA synthesis kit (Thermo Fisher-Verso cDNA Synthesis Kit; Cat no: AB1453B) according to the manufacturer's protocol. Finally, cDNA concentration is measured by using a nanodrop spectrophotometer in ng/μl. For RNA isolation, we have taken 2000 worms at L4 stage for each group and the experiment and repeated it three times.

5.10. Quantitative real-time PCR assay

Amplified cDNA quantitative assessment was done by using SYBR Green dye (Thermo Scientific Cat. No. K0251) and according to the manual protocol by the manufacturer, all qPCR experiments were performed by the manufacturer. Briefly, 100 ng of cDNA was amplified using a thermal cycler detection system (Agilent Technologies-MX3005P). The amplification conditions were: pre-incubation cycle (Total 1 cycle for 2 min at 50 °C and for 10 min at 95 °C) which is followed by 40 amplification cycles o (for 30 s at 95 °C, for 30 s at 55 °C, and for 30 s at 60 °C) and to generate melting curve (95 °C for 5 s, 65 °C for 1 min). Each q-PCR experiment was performed at least twice in replicates. We have normalized the ct values of each gene with actin (*act-1*) as an endogenous control.

5.11. Lifespan assay

Isolated embryos of desired *C. elegans* strains were applied on both treated and control plates to obtain age-synchronized worms. After 48 h, onto freshly prepared feeding plates of treatment control and groups, under stereo zoom microscope, one hundred adult worms (L4 stage) were picked and transferred respectively. From that day onwards, daily scoring of live, dead, and censored worms was performed; two plates for each group is used for scoring. A censored set of data was recorded based on the total number of missing worms or the desiccated worms near the plates' edge. Based on the feedback response to gentle prodding on the head of worms, live, and dead worms were identified. The worm was considered dead if no response is observed. On a daily basis for 20 days, the nematodes were transferred onto fresh feeding plates which were maintained at 22 °C using BOD incubators that we employ for rearing of the worms. The scoring of worms was performed from egg till its death, and data was analyzed by Kaplan Meier survival curve.

5.12. Gene network analysis

We used GeneMANIA (Gene Multiple Association Network Integration Algorithm), a free accessible and user-friendly web tool for the retrieval of interacting genes/proteins (http://www.genemania.org, Application version: 3.1.2.8). Genes were represented as “node”, while the interactions between the genes were represented as an “edge”. Based on query gene, it shows results for an interactive functional associative network according to their; Genetic and Physical interaction data derived from BioGRID.

5.13. Autophagy and proteasome inhibition

For Autophagy inhibition, we have used 10 mM of 3-Methyl Adenine

(3-MA), and for proteasome inhibition, we have used 50 μM of MG132. The inhibitors are seeded with the culture overnight at 22 °C at BOD and used in the next day to put isolated embryos on it.

5.14. Statistical method and control for the experiments

For microscopy-based quantification assays, we have carried out at least two independent experiments treating and studying over 100 worms for each group. Whereas the fluorescence intensity of worms is observed for the entire set of slides, the representative images are grabbed for $n = 10$ within each individual experiment. Wherever two independent experiments are conducted, we end up studying the fluorescence pattern in 100–200 worms and record images for at least $n = 20$. These images are then processed for quantification of intensity using Image J analysis.

To analyze statistically quantified fluorescent images, ROS values from luminometer, Number of thrashes of worms and dopamine content and the ct values obtained from qPCR methods we have followed non-parametric independent 't' test using Prism 5 software, where *p*-value is represented as; $*p < 0.05$, $**p < 0.005$ $***p < 0.0005$ & ns: non-significant.

Across all experiments, we have used adult worms at L4 stage. For the control groups, we have used an empty vector (EV) with respect to which we have accessed the phenotypic, behavioral or genetic modulations in the *C. elegans.*

5.15. Isolation of small non-coding RNAs using mirVana™ miRNA isolation kit

The standard protocol was employed for the extraction of small non-coding RNAs; briefly, 0.2 % diethylpyrocarbonate (DEPC-Sigma, Cat. No.-D5758) treated water was used to remove adhering bacteria from age synchronized control and treated groups. The mirVana™miRNA isolation kit (Ambion P/N AM1561) was used for the isolation of miRNAs. According to protocol 250 μl lysis/binding buffer was added worms were homogenized in lysis buffer followed by the addition of 1/10 miRNA homogenate additive; the solution was mixed gently and kept on ice for 10 mins. After this step, to the lysate, an equal amount of Acid-phenol: chloroform was added and centrifuged for 5 mins at 10,000*g. After centrifugation, the aqueous phase was removed and 1.25 times the volume of absolute ethanol was added after this step, filtration was done by passing through the filter cartridge, washing and elution.

5.16. Reverse transcriptase reaction

cDNA was prepared from isolated non-coding small RNAs using MicroRNA Reverse Transcription TaqMan® kit (Applied Biosystem cat no. P/N 4366596). For reaction, 10 ng noncoding RNA (template), 1 μl multiscribe RT enzyme (50 U/μl), 1.5 μl 10X RT buffer, 0.19 μl RNase inhibitor (20 U/μl), 3 μl specific miRNA primer were added into PCR microcentrifuge tube. Gently vortexed the reaction mixture and processed using Agilent sure Cycler 8800 at 16 °C for 30 min, at 42 °C for 30 min, at 85 °C 5 min and then held at 4 °C.

5.17. TaqMan miRNA assay

miRNA quantification was carried out using Universal Master MixII TaqMan® MixII (Applied Biosystem cat no. 4440040). 100 ng cDNA template and 1X TaqMan® Universal Master MixII were mixed together to prepare the reaction mixture. The amplification program was 95 °C for 10 min (for1 cycle), then by 95 °C for 15 s and finally 60 °C for 1 min (for 40 cycles) run into 3005P-Agilent. The experiment was carried out in triplicate sets for each sample. Fold change of all the samples were evaluated using comparative $2^{-\Delta\Delta CT}$ [99,100,107,108]. For normalization of miRNA expression U18 was used as an endogenous control.

5.18. Non-coding small RNA library preparation for next-generation sequencing (NGS)

1 μg of total RNA was used as the starting material and 3′ adaptors were ligated to the specific 3'OH group of miRNAs followed by 5′ adaptor ligation. Superscript III Reverse transcriptase was used for the reverse transcription of miRNA ligated products by priming with Reverse transcriptase primers. The cDNA was enriched and barcoded by PCR (15 cycles) and cleaned using Poly-acrylamide gel. 140–160 bp range of size was selected for the library followed by overnight gel elution. Salt was precipitated using Glycogen, 3 M Sodium Acetate and Absolute Ethanol and re-suspended in Nuclease-free water. The prepared library was quantified using Qubit Fluorometer and validated for quality by running an aliquot on a High Sensitivity Bioanalyzer Chip (Agilent).

5.19. Analysis of miRNAome data

Srna-workbenchV3.0_ALPHA was used to trim the Trueseq adapter sequences and perform length range filtering [109]. Sequence length of >16 bp and <36 bp were appraised for further analysis. *C. elegans* GRCh38 genome build used for the sequence alignment and Aligned reads were extracted and checked for ncRNA (rRNA, tRNA, snRNA and snoRNA) contamination. The unaligned reads in ncRNAs were considered as known miRNAs. Reads were made unique and hence read count profile was generated. *C. elegans*mature miRNA sequences retrieved from miRbase-21 [110] and miRNAs homology search were done by NCBI -blast-2.2.30+ [111]. Sequence-matched reported for known miRNAs and showing no hits with known miRNAs were predicted as novel miRNAs, done by Mireap_0.2. Differential Gene Expression (DGE) analysis was carried out using DESeq [112] tool and for reference, *C. elegans* genome sequence was used.

Abbreviations

PD	Parkinson's Disease
PQC	Protein Quality Control
ROS	Reactive Oxygen Species
NDs	Neurodegenerative Diseases
UPR	Unfolded Protein Response
AD	Alzheimer's disease
ISF	interstitial fluid
CSF	Cerebrospinal fluid
qPCR	Quantitative Polymerase Chain Reaction
SOD2	Super Oxide Dismutase 2
ALP	autophagosome-lysosomal-pathway
UPS	Ubiquitin Proteasomal System
CPM	carboxypeptidase
NCS-1	Neuronal calcium Sensor-1
TNF	Tumor Necrosis Factor
CPE	Carboxy Peptidase E
TRP	Transient Receptor Potential
TAG	Triacyl Glycerol
ASK	apoptosis signal-regulating kinase
MAPK	MAP kinase
(ko)	Knock Out
ER^{UPR}	Endoplasmic reticulum unfolded protein response
MT^{UPR}	Mitochondrial unfolded protein response
BOD	Biological Oxygen Demand
Alpha-synuclein	α-synuclein
micro RNA	miRNA

Supplementary data to this article can be found online at https://doi.org/10.1016/j.bbamcr.2022.119342.

Funding source

AS is Senior Research Fellow (CSIR) vide reference no EMR/No./31/004(1273)2014-EMR-I. AN acknowledges funding received from CSIR vide project MLP2030 (unCIDAN) and institutional project MLP0020 (Neuroscience and Aging Biology).

CRediT authorship contribution statement

AS conducted the experiments, analyzed data, wrote the manuscript, RH, S and LK contributed in conducting some of the experiments and towards analyzing data; AN conceived the study, provided infrastructure and reagents, analyzed the data and edited the manuscript.

Data availability statement

The data that support the findings of this study are available from the corresponding author upon reasonable request.

Declaration of competing interest

All authors read the manuscript and agreed its content before the submission. The authors declare no competing interest.

Data availability

Data will be made available on request.

Acknowledgement

We are thankful to the Caenorhabditis Genetics Center (CGC), University of Minnesota, MN, USA, for providing the *C. elegans* strains. Contribution of Dr. Malathi Srinivasan in thorough proof-reading and editing of the manuscript is acknowledged. CSIR-CDRI communication number is 10448.

We also want to thank Ms. Anjali Mishra and Dr. Rabi Sankar Bhatta for helping us in the quantification of dopamine levels during our experiments.

References

[1] S.A. Luse, K.R. Smith, The ultrastructure of senile plaques, Am. J. Pathol. 44 (1964) 553–563.
[2] V. Liang, M. Ullrich, H. Lam, Y.L. Chew, S. Banister, X. Song, T. Zaw, M. Kassiou, J. Götz, H.R. Nicholas, Altered proteostasis in aging and heat shock response in C. Elegans revealed by analysis of the global and de novo synthesized proteome, Cell. Mol. Life Sci. 71 (2014) 3339–3361, https://doi.org/10.1007/s00018-014-1558-7.
[3] S. Shao, R.S. Hegde, Target selection during protein quality control, Trends Biochem. Sci. 41 (2016) 124–137, https://doi.org/10.1016/j.tibs.2015.10.007.
[4] F. Chiti, C.M. Dobson, Protein misfolding, amyloid formation, and human disease: a summary of progress over the last decade, Annu. Rev. Biochem. 86 (2017) 27–68, https://doi.org/10.1146/annurev-biochem-061516-045115.
[5] E.T. Powers, R.I. Morimoto, A. Dillin, J.W. Kelly, W.E. Balch, Biological and chemical approaches to diseases of proteostasis deficiency, Annu. Rev. Biochem. 78 (2009) 959–991, https://doi.org/10.1146/annurev.biochem.052308.114844.
[6] A. Sarkar, A. Nazir, Carrying excess baggage can slowdown life: protein clearance machineries that go awry during aging and the relevance of maintaining them, Mol. Neurobiol. 59 (2022) 821–840, https://doi.org/10.1007/s12035-021-02640-2.
[7] M. Selbach, B. Schwanhäusser, N. Thierfelder, Z. Fang, R. Khanin, N. Rajewsky, Widespread changes in protein synthesis induced by microRNAs, Nature 455 (2008) 58–63, https://doi.org/10.1038/nature07228.
[8] I. Bicchi, F. Morena, S. Montesano, M. Polidoro, S. Martino, MicroRNAs and molecular mechanisms of neurodegeneration, Genes (Basel) 4 (2013) 244–263, https://doi.org/10.3390/genes4020244.
[9] A.M. Krichevsky, K.S. King, C.P. Donahue, K. Khrapko, K.S. Kosik, Erratum: a microRNA array reveals extensive regulation of microRNAs during brain development (RNA (2003) 9 (1274–1281)), RNA 10 (2004) 551, https://doi.org/10.1261/rna.5980303.regulation.
[10] L.F. Sempere, S. Freemantle, I. Pitha-Rowe, E. Moss, E. Dmitrovsky, V. Ambros, Expression profiling of mammalian microRNAs uncovers a subset of brain-expressed microRNAs with possible roles in murine and human neuronal differentiation, Genome Biol. 5 (2004), https://doi.org/10.1186/gb-2004-5-3-r13.
[11] G.M. Schratt, F. Tuebing, E.A. Nigh, C.G. Kane, M.E. Sabatini, M. Kiebler, M. E. Greenberg, A brain-specific microRNA regulates dendritic spine development, Nature 439 (2006) 283–289, https://doi.org/10.1038/nature04367.
[12] C.T. Lee, T. Risom, W.M. Strauss, MicroRNAs in mammalian development, Birth Defects Res. C. Embryo Today 78 (2006) 129–139, https://doi.org/10.1002/bdrc.20072.
[13] Y. Lu, J.M. Thomson, H.Y.F. Wong, S.M. Hammond, B.L.M. Hogan, Transgenic over-expression of the microRNA miR-17-92 cluster promotes proliferation and inhibits differentiation of lung epithelial progenitor cells, Dev. Biol. 310 (2007) 442–453, https://doi.org/10.1016/j.ydbio.2007.08.007.
[14] M. Kumar, S. Nath, H.K. Prasad, G.D. Sharma, Y. Li, MicroRNAs: a new ray of hope for diabetes mellitus, Protein Cell 3 (2012) 726–738, https://doi.org/10.1007/s13238-012-2055-0.
[15] S. Dimmeler, P. Nicotera, MicroRNAs in age-related diseases, EMBO Mol. Med. 5 (2013) 180–190, https://doi.org/10.1002/emmm.201201986.
[16] J. Kocerha, Y. Xu, M.S. Prucha, D. Zhao, A.W.S. Chan, MicroRNA-128a dysregulation in transgenic Huntington's disease monkeys, Mol. Brain 7 (2014) 1–10, https://doi.org/10.1186/1756-6606-7-46.
[17] K. Tsukita, H. Sakamaki-Tsukita, K. Tanaka, T. Suenaga, R. Takahashi, Value of in vivo α-synuclein deposits in Parkinson's disease: a systematic review and meta-analysis, Mov. Disord. 34 (2019) 1452–1463, https://doi.org/10.1002/mds.27794.
[18] J.R. Patterson, M.F. Duffy, C.J. Kemp, J.W. Howe, T.J. Collier, A.C. Stoll, K. M. Miller, P. Patel, N. Levine, D.J. Moore, K.C. Luk, S.M. Fleming, N.M. Kanaan, K.L. Paumier, O.M.A. El-Agnaf, C.E. Sortwell, Time course and magnitude of alpha-synuclein inclusion formation and nigrostriatal degeneration in the rat model of synucleinopathy triggered by intrastriatal α-synuclein preformed fibrils, Neurobiol. Dis. 130 (2019), https://doi.org/10.1016/j.nbd.2019.104525.
[19] D. Caligiore, F. Mannella, G. Baldassarre, Different dopaminergic dysfunctions underlying parkinsonian akinesia and tremor, Front. Neurosci. 13 (2019) 1–15, https://doi.org/10.3389/fnins.2019.00550.
[20] G.Q. Wang, Y.Z. Zhou, Y.Y. Wang, D. Li, J. Liu, F. Zhang, Age-associated dopaminergic neuron loss and midbrain glia cell phenotypic polarization, Neuroscience 415 (2019) 89–96, https://doi.org/10.1016/j.neuroscience.2019.07.021.
[21] L. Cai, L. Tu, T. Li, X. Yang, Y. Ren, R. Gu, Q. Zhang, H. Yao, X. Qu, Q. Wang, J. Tian, Downregulation of lncRNA UCA1 ameliorates the damage of dopaminergic neurons, reduces oxidative stress and inflammation in Parkinson's disease through the inhibition of the PI3K/Akt signaling pathway, Int. Immunopharmacol. 75 (2019), https://doi.org/10.1016/j.intimp.2019.105734.
[22] J.M. Froula, M. Castellana-Cruz, N.M. Anabtawi, J.D. Camino, S.W. Chen, D. R. Thrasher, J. Freire, A.A. Yazdi, S. Fleming, C.M. Dobson, J.R. Kumita, N. Cremades, L.A. Volpicelli-Daley, Defining α-synuclein species responsible for Parkinson's disease phenotypes in mice, J. Biol. Chem. 294 (2019) 10392–10406, https://doi.org/10.1074/jbc.RA119.007743.
[23] S.N. Jacob, H. Nienborg, Monoaminergic neuromodulation of sensory processing, Front. Neural Circ. 12 (2018) 1–17, https://doi.org/10.3389/fncir.2018.00051.
[24] S. Reinig, W. Driever, A.B. Arrenberg, The descending diencephalic dopamine system is tuned to sensory stimuli, Curr. Biol. 27 (2017) 318–333, https://doi.org/10.1016/j.cub.2016.11.059.
[25] N. Wolpe, J. Zhang, C. Nombela, J.N. Ingram, D.M. Wolpert, J.B. Rowe, L. K. Tyler, C. Brayne, E.T. Bullmore, A.C. Calder, R. Cusack, T. Dalgleish, J. Duncan, F.E. Matthews, W.D. Marslen-Wilson, M.A. Shafto, T. Cheung, L. Geerligs, A. McCarrey, A. Mustafa, D. Price, D. Samu, M. Treder, K. A. Tsvetanov, J. van Belle, N. Williams, L. Bates, A. Gadie, S. Gerbase, S. Georgieva, C. Hanley, B. Parkin, D. Troy, T. Auer, M. Correia, L. Gao, E. Green, R. Henriques, J. Allen, G. Amery, L. Amunts, A. Barcroft, A. Castle, C. Dias, J. Dowrick, M. Fair, H. Fisher, A. Goulding, A. Grewal, G. Hale, A. Hilton, F. Johnson, P. Johnston, T. Kavanagh-Williamson, M. Kwasniewska, A. McMinn, K. Norman, J. Penrose, F. Roby, D. Rowland, J. Sargeant, M. Squire, B. Stevens, A. Stoddart, C. Stone, T. Thompson, O. Yazlik, M. Dan Barnes, J. Dixon, J. Hillman, L.Villis Mitchell, Sensory attenuation in Parkinson's disease is related to disease severity and dopamine dose, Sci. Rep. 8 (2018) 1–10, https://doi.org/10.1038/s41598-018-33678-3.
[26] J.G. Nutt, J.H. Carter, G.J. Sexton, The dopamine transporter: importance in Parkinson's disease, Ann. Neurol. 55 (2004) 766–773, https://doi.org/10.1002/ana.20089.
[27] M.L. Arotcarena, M. Teil, B. Dehay, Autophagy in synucleinopathy: the overwhelmed and defective machinery, Cells 8 (2019) 1–24, https://doi.org/10.3390/cells8060565.
[28] T. Meng, S. Lin, H. Zhuang, H. Huang, Z. He, Y. Hu, Q. Gong, D. Feng, Recent progress in the role of autophagy in neurological diseases, Cell Stress 3 (2019) 141–161, https://doi.org/10.15698/cst2019.05.186.
[29] X.H. Zhao, Y.B. Wang, J. Yang, H.Q. Liu, L.L. Wang, MicroRNA-326 suppresses iNOS expression and promotes autophagy of dopaminergic neurons through the JNK signaling by targeting XBP1 in a mouse model of Parkinson's disease, J. Cell. Biochem. 120 (2019) 14995–15006, https://doi.org/10.1002/jcb.28761.
[30] J. Lim, Z. Yue, Neuronal aggregates: formation, clearance, and spreading, Dev. Cell 32 (2015) 491–501, https://doi.org/10.1016/j.devcel.2015.02.002.
[31] N. Ramesh, U.B. Pandey, Autophagy dysregulation in ALS: when protein aggregates get out of hand, Front. Mol. Neurosci. 10 (2017) 1–18, https://doi.org/10.3389/fnmol.2017.00263.
[32] J.M.T. Hyttinen, M. Amadio, J. Viiri, A. Pascale, A. Salminen, K. Kaarniranta, Clearance of misfolded and aggregated proteins by aggrephagy and implications

for aggregation diseases, Ageing Res. Rev. 18 (2014) 16–28, https://doi.org/10.1016/j.arr.2014.07.002.
[33] K. Takacs-Vellai, T. Vellai, A. Puoti, M. Passannante, C. Wicky, A. Streit, A. L. Kovacs, F. Müller, Inactivation of the autophagy gene bec-1 triggers apoptotic cell death in C. Elegans, Curr. Biol. 15 (2005) 1513–1517, https://doi.org/10.1016/j.cub.2005.07.035.
[34] G. Fazeli, M. Trinkwalder, L. Irmisch, A.M. Wehman, C. elegans midbodies are released, phagocytosed and undergo LC3-dependent degradation independent of macroautophagy, J. Cell Sci. 129 (2016) 3721–3731, https://doi.org/10.1242/jcs.190223.
[35] S. Cheng, Y. Wu, Q. Lu, J. Yan, H. Zhang, X. Wang, Autophagy genes coordinate with the class II PI/PtdIns 3-kinase PIKI-1 to regulate apoptotic cell clearance in C. Elegans, Autophagy 9 (2013) 2022–2032, https://doi.org/10.4161/auto.26323.
[36] A. Alberti, X. Michelet, A. Djeddi, R. Legouis, The autophagosomal protein LGG-2 acts synergistically with LGG-1 in dauer formation and longevity in C. Elegans, Autophagy 6 (2010) 622–633, https://doi.org/10.4161/auto.6.5.12252.
[37] Characterization of Class I and II ADP-ribosylation factors, (Arfs) in live cells: GDP-bound Class II Arfs associate, with the E.-G.I.C. Independently, O. GBF1, 乳鼠心肌提取 HHS public access, Physiol. Behav. 176 (2017) 139–148, https://doi.org/10.1111/febs.14970.Apoptotic.
[38] F. Cecconi, G. Alvarez-Bolado, B.I. Meyer, K.A. Roth, P. Gruss, Apaf1 (CED-4 homolog) regulates programmed cell death in mammalian development, Cell 94 (1998) 727–737, https://doi.org/10.1016/S0092-8674(00)81732-8.
[39] T. Hayakawa, K. Kato, R. Hayakawa, N. Hisamoto, K. Matsumoto, K. Takeda, H. Ichijo, Regulation of anoxic death in Caenorhabditis elegans by mammalian apoptosis signal-regulating kinase (ASK) family proteins, Genetics 187 (2011) 785–792, https://doi.org/10.1534/genetics.110.124883.
[40] Z. Yue, L. Friedman, M. Komatsu, K. Tanaka, The cellular pathways of neuronal autophagy and their implication in neurodegenerative diseases, Biochim. Biophys. Acta - Mol. Cell Res. 1793 (2009) 1496–1507, https://doi.org/10.1016/j.bbamcr.2009.01.016.
[41] W. Huang, T. Jiang, W. Choi, S. Qi, Y. Pang, Q. Hu, Y. Xu, X. Gong, P.D. Jeffrey, J. Wang, Y. Shi, Mechanistic insights into CED-4-mediated activation of CED-3, Genes Dev. 27 (2013) 2039–2048, https://doi.org/10.1101/gad.224428.113.
[42] D.N. Dhanasekaran, E.P. Reddy, JNK signaling in apoptosis, Oncogene 27 (2008) 6245–6251, https://doi.org/10.1038/onc.2008.301.
[43] M. Kawasaki, N. Hisamoto, Y. Lino, M. Yamamoto, J. Ninomiya-Tsuji, K. Matsumoto, A Caenorhabditis elegans JNK signal transduction pathway regulates coordinated movement via type-D GABAergic motor neurons, EMBO J. 18 (1999) 3604–3615, https://doi.org/10.1093/emboj/18.13.3604.
[44] R.E. Musgrove, M. Helwig, E.J. Bae, H. Aboutalebi, S.J. Lee, A. Ulusoy, D.A. Di Monte, Oxidative stress in vagal neurons promotes parkinsonian pathology and intercellular α-synuclein transfer, J. Clin. Invest. 129 (2019) 3738–3753, https://doi.org/10.1172/JCI127330.
[45] A. Krishnamoorthy, M. Sevanan, S. Mani, M. Balu, S. Balaji, R. P, Chrysin restores MPTP induced neuroinflammation, oxidative stress and neurotrophic factors in an acute Parkinson's disease mouse model, Neurosci. Lett. 709 (2019), 134382, https://doi.org/10.1016/j.neulet.2019.134382.
[46] R. Stefanatos, A. Sanz, The role of mitochondrial ROS in the aging brain, FEBS Lett. 592 (2018) 743–758, https://doi.org/10.1002/1873-3468.12902.
[47] H.J. van Heesbeen, M.P. Smidt, Entanglement of genetics and epigenetics in Parkinson's disease, Front. Neurosci. 13 (2019) 1–15, https://doi.org/10.3389/fnins.2019.00277.
[48] F.Q.N. Ameliorates, C.C. Lines, in: Food-Grade Quercetin-Loaded Nanoemulsion Ameliorates Effects Associated with Parkinson ' s Disease and Cancer : Studies Employing a Transgenic C . elegans Model and Human Cancer Cell Lines, 2022, pp. 1–14.
[49] A. Sarkar, R. Hameed, A. Mishra, R.S. Bhatta, A. Nazir, Genetic modulators associated with regulatory surveillance of mitochondrial quality control, play a key role in regulating stress pathways and longevity in C. Elegans, Life Sci. 290 (2022), 120226, https://doi.org/10.1016/j.lfs.2021.120226.
[50] P. Davalli, T. Mitic, A. Caporali, A. Lauriola, D. D'Arca, ROS, cell senescence, and novel molecular mechanisms in aging and age-related diseases, Oxidative Med. Cell. Longev. 2016 (2016), https://doi.org/10.1155/2016/3565127.
[51] K.B. Ackema, U. Sauder, J.A. Solinger, A. Spang, The ArfGEF GBF-1 is required for ER structure, secretion and endocytic transport in C. Elegans, PLoS One 8 (2013), https://doi.org/10.1371/journal.pone.0067076.
[52] J.R.M.Sophie Mokas, M.-J.Cristina Garreau, é Fournier, F. Robert, P. Arya, R. J. Kaufman, J. Pelletier, R. Mazroui, Molecular biology of the cell vol. 19, 3488–3500, August 200, Mol. Biol. Cell. 20 (2009) 2673–2683, https://doi.org/10.1091/mbc.E08.
[53] K.B. Ackema, J. Hench, S. Böckler, S.C. Wang, U. Sauder, H. Mergentaler, B. Westermann, F. Bard, S. Frank, A. Spang, The small GTP ase Arf1 modulates mitochondrial morphology and function, EMBO J. 33 (2014) 2659–2675, https://doi.org/10.15252/embj.201489039.
[54] Version of record. https://www.sciencedirect.com/science/article/pii/S0969996117302723, 2017.
[55] D.C. Schöndorf, M. Aureli, F.E. McAllister, C.J. Hindley, F. Mayer, B. Schmid, S. P. Sardi, M. Valsecchi, S. Hoffmann, L.K. Schwarz, U. Hedrich, D. Berg, L. S. Shihabuddin, J. Hu, J. Pruszak, S.P. Gygi, S. Sonnino, T. Gasser, M. Deleidi, IPSC-derived neurons from GBA1-associated Parkinson's disease patients show autophagic defects and impaired calcium homeostasis, Nat. Commun. 5 (2014), https://doi.org/10.1038/ncomms5028.
[56] J.H. Choi, B. Stubblefield, M.R. Cookson, E. Goldin, A. Velayati, N. Tayebi, E. Sidransky, Aggregation of α-synuclein in brain samples from subjects with glucocerebrosidase mutations, Mol. Genet. Metab. 104 (2011) 185–188, https://doi.org/10.1016/j.ymgme.2011.06.008.
[57] V. Cullen, S.P. Sardi, J. Ng, Y.H. Xu, Y. Sun, J.J. Tomlinson, P. Kolodziej, I. Kahn, P. Saftig, J. Woulfe, J.C. Rochet, M.A. Glicksman, S.H. Cheng, G.A. Grabowski, L. S. Shihabuddin, M.G. Schlossmacher, Acid β-glucosidase mutants linked to gaucher disease, parkinson disease, and lewy body dementia alter α-synuclein processing, Ann. Neurol. 69 (2011) 940–953, https://doi.org/10.1002/ana.22400.
[58] L.D. Osellame, A.A. Rahim, I.P. Hargreaves, M.E. Gegg, A. Richard-Londt, S. Brandner, S.N. Waddington, A.H.V. Schapira, M.R. Duchen, Mitochondria and quality control defects in a mouse model of gaucher disease - links to parkinson's disease, Cell Metab. 17 (2013) 941–953, https://doi.org/10.1016/j.cmet.2013.04.014.
[59] W. Li, T. Nie, H. Xu, J. Yang, Q. Yang, Z. Mao, Chaperone-mediated autophagy: advances from bench to bedside, Neurobiol. Dis. 122 (2019) 41–48, https://doi.org/10.1016/j.nbd.2018.05.010.
[60] T. Sun, X. Wang, Q. Lu, H. Ren, H. Zhang, CUP-5, the C. Elegans ortholog of the mammalian lysosomal channel protein MLN1/TRPML1, is required for proteolytic degradation in autolysosomes, Autophagy 7 (2011) 1308–1315, https://doi.org/10.4161/auto.7.11.17759.
[61] E.M. Campbell, H. Fares, Roles of CUP-5, the Caenorhabditis elegans orthologue of human TRPML1, in lysosome and gut granule biogenesis, BMC Cell Biol. 11 (2010), https://doi.org/10.1186/1471-2121-11-40.
[62] L. Schaheen, G. Patton, H. Fares, Suppression of the cup-5 mucolipidosis type IV-related lysosomal dysfunction by the inactivation of an ABC transporter in C. Elegans, Development 133 (2006) 3939–3948, https://doi.org/10.1242/dev.02575.
[63] B.M. Hersh, E. Hartwieg, H.R. Horvitz, The Caenorhabditis elegans mucolipin-like gene cup-5 is essential for viability and regulates lysosomes in multiple cell types, Proc. Natl. Acad. Sci. U. S. A. 99 (2002) 4355–4360, https://doi.org/10.1073/pnas.062065399.
[64] D. Ramonet, A. Podhajska, K. Stafa, S. Sonnay, A. Trancikova, E. Tsika, O. Pletnikova, J.C. Troncoso, L. Glauser, D.J. Moore, PARK9-associated ATP13A2 localizes to intracellular acidic vesicles and regulates cation homeostasis and neuronal integrity, Hum. Mol. Genet. 21 (2012) 1725–1743, https://doi.org/10.1093/hmg/ddr606.
[65] A. Grünewald, B. Arns, P. Seibler, A. Rakovic, A. Münchau, A. Ramirez, C.M. Sue, C. Klein, ATP13A2 mutations impair mitochondrial function in fibroblasts from patients with kufor-rakeb syndrome, Neurobiol. Aging 33 (2012) (1843) e1–1843.e7, https://doi.org/10.1016/j.neurobiolaging.2011.12.035.
[66] M. Kniazeva, H. Shen, T. Eule, C. Wang, M. Han, Regulation of maternal phospholipid composition and IP 3-dependent embryonic membrane dynamics by a specific fatty acid metabolic event in C.Elegans, Genes Dev. 26 (2012) 554–566, https://doi.org/10.1101/gad.187054.112.
[67] J. Zhang, R. Bakheet, R.S. Parhar, C.H. Huang, M.M. Hussain, X. Pan, S. S. Siddiqui, S. Hashmi, Regulation of fat storage and reproduction by Krüppel-like transcription factor KLF3 and fat-associated genes in Caenorhabditis elegans, J. Mol. Biol. 411 (2011) 537–553, https://doi.org/10.1016/j.jmb.2011.06.011.
[68] S. Kaushik, A.M. Cuervo, Proteostasis and aging, Nat. Med. 21 (2015) 1406–1415, https://doi.org/10.1038/nm.4001.
[69] L. Shamsuzzama, A.Nazir Kumar, Modulation of alpha-synuclein expression and associated effects by microRNA let-7 in transgenic C. Elegans, Front. Mol. Neurosci. 10 (2017) 1–14, https://doi.org/10.3389/fnmol.2017.00328.
[70] M.A. Parasramka, W.M. Dashwood, R. Wang, H.H. Saeed, D.E. Williams, E. Ho, R. H. Dashwood, A role for low-abundance miRNAs in colon cancer: the miR-206/Krüppel-like factor 4 (KLF4) axis, Clin. Epigenetics 4 (2012) 1–10, https://doi.org/10.1186/1868-7083-4-16.
[71] M. Gómez-Benito, N. Granado, P. García-Sanz, A. Michel, M. Dumoulin, R. Moratalla, Modeling Parkinson's disease with the alpha-synuclein protein, Front. Pharmacol. 11 (2020) 1–15, https://doi.org/10.3389/fphar.2020.00356.
[72] C.R. Fields, N. Bengoa-Vergniory, R. Wade-Martins, Targeting alpha-synuclein as a therapy for Parkinson's disease, Front. Mol. Neurosci. 12 (2019) 1–14, https://doi.org/10.3389/fnmol.2019.00299.
[73] A. Martinez, N. Lopez, C. Gonzalez, C. Hetz, Targeting of the unfolded protein response (UPR) as therapy for Parkinson's disease, Biol. Cell. 111 (2019) 161–168, https://doi.org/10.1111/boc.201800068.
[74] S. Franco-Iborra, M. Vila, C. Perier, Mitochondrial quality control in neurodegenerative diseases: focus on Parkinson's disease and Huntington's disease, Front. Neurosci. 12 (2018) 1–25, https://doi.org/10.3389/fnins.2018.00342.
[75] M. Bourdenx, J. Daniel, E. Genin, F.N. Soria, M. Blanchard-Desce, E. Bezard, B. Dehay, Nanoparticles restore lysosomal acidification defects: implications for parkinson and other lysosomal-related diseases, Autophagy 12 (2016) 472–483, https://doi.org/10.1080/15548627.2015.1136769.
[76] T.E. Moors, S. Paciotti, A. Ingrassia, M. Quadri, G. Breedveld, A. Tasegian, D. Chiasserini, P. Eusebi, G. Duran-Pacheco, T. Kremer, P. Calabresi, V. Bonifati, L. Parnetti, T. Beccari, W.D.J. van de Berg, Characterization of brain lysosomal activities in GBA-related and sporadic Parkinson's disease and dementia with lewy bodies, Mol. Neurobiol. 56 (2019) 1344–1355, https://doi.org/10.1007/s12035-018-1090-0.
[77] B. editing: precision chemistry on the genome and, transcriptome of living cells, 乳鼠心肌提取 HHS public access, Physiol. Behav. 176 (2016) 139–148, https://doi.org/10.1016/j.nbd.2017.11.006.The.
[78] T. Calì, D. Ottolini, M. Brini, Calcium signaling in Parkinson's disease, Cell Tissue Res. 357 (2014) 439–454, https://doi.org/10.1007/s00441-014-1866-0.

[79] T. Moors, S. Paciotti, D. Chiasserini, P. Calabresi, L. Parnetti, T. Beccari, W.D. J. van de Berg, Lysosomal dysfunction and α-synuclein aggregation in Parkinson's disease: diagnostic links, Mov. Disord. 31 (2016) 791–801, https://doi.org/10.1002/mds.26562.
[80] T. Fukuzono, S.I. Pastuhov, O. Fukushima, C. Li, A. Hattori, S. Ichiro Iemura, T. Natsume, H. Shibuya, H. Hanafusa, K. Matsumoto, N. Hisamoto, Chaperone complex BAG2-HSC70 regulates localization of Caenorhabditis elegans leucine-rich repeat kinase LRK-1 to the Golgi, Genes Cells 21 (2016) 311–324, https://doi.org/10.1111/gtc.12338.
[81] M.K. Tripathi, C. Rajput, S. Mishra, M.S. Ur Rasheed, M.P. Singh, Malfunctioning of chaperone-mediated autophagy in Parkinson's disease: feats, constraints, and flaws of modulators, Neurotox. Res. 35 (2019) 260–270, https://doi.org/10.1007/s12640-018-9917-z.
[82] D.J. Eisermann, U. Wenzel, E. Fitzenberger, Inhibition of chaperone-mediated autophagy prevents glucotoxicity in the Caenorhabditis elegans mev-1 mutant by activation of the proteasome, Biochem. Biophys. Res. Commun. 484 (2017) 171–175, https://doi.org/10.1016/j.bbrc.2017.01.043.
[83] L.L. Venda, S.J. Cragg, V.L. Buchman, R. Wade-Martins, α-synuclein and dopamine at the crossroads of Parkinson's disease, Trends Neurosci. 33 (2010) 559–568, https://doi.org/10.1016/j.tins.2010.09.004.
[84] C. McKinnon, M.L. De Snoo, E. Gondard, C. Neudorfer, H. Chau, S.G. Ngana, D. M. O'Hara, J.M. Brotchie, J.B. Koprich, A.M. Lozano, L.V. Kalia, S.K. Kalia, Early-onset impairment of the ubiquitin-proteasome system in dopaminergic neurons caused by α-synuclein, Acta Neuropathol. Commun. 8 (2020) 1–16, https://doi.org/10.1186/s40478-020-0894-0.
[85] E. Bentea, L. Verbruggen, A. Massie, The proteasome inhibition model of Parkinson's disease, J. Parkinsons. Dis. 7 (2017) 31–63, https://doi.org/10.3233/JPD-160921.
[86] G.K. Tofaris, A. Razzaq, B. Ghetti, K.S. Lilley, M.G. Spillantini, Ubiquitination of α-synuclein in lewy bodies is a pathological event not associated with impairment of proteasome function, J. Biol. Chem. 278 (2003) 44405–44411, https://doi.org/10.1074/jbc.M308041200.
[87] F.R. Lin, J.K. Niparko, L. Ferrucci, 基因的改变NIH Public Access, 2014, https://doi.org/10.1016/j.freeradbiomed.2013.05.001.Glutathione.
[88] Donahoe, 基因的改变NIH public access, Mol. Cell. Biochem. 23 (2012) 1–7, https://doi.org/10.1016/j.freeradbiomed.2012.11.014.Mitochondrial.
[89] A. Umeno, V. Biju, Y. Yoshida, In vivo ROS production and use of oxidative stress-derived biomarkers to detect the onset of diseases such as Alzheimer's disease, Parkinson's disease, and diabetes, Free Radic. Res. 51 (2017) 413–427, https://doi.org/10.1080/10715762.2017.1315114.
[90] K. Bartel, H. Pein, B. Popper, S. Schmitt, S. Janaki-Raman, A. Schulze, F. Lengauer, A. Koeberle, O. Werz, H. Zischka, R. Müller, A.M. Vollmar, K. Von Schwarzenberg, Connecting lysosomes and mitochondria - a novel role for lipid metabolism in cancer cell death, Cell Commun. Signal. 17 (2019) 1–16, https://doi.org/10.1186/s12964-019-0399-2.
[91] X. Zhang, X. Cheng, L. Yu, J. Yang, R. Calvo, S. Patnaik, X. Hu, Q. Gao, M. Yang, M. Lawas, M. Delling, J. Marugan, M. Ferrer, H. Xu, MCOLN1 is a ROS sensor in lysosomes that regulates autophagy, Nat. Commun. 7 (2016), https://doi.org/10.1038/ncomms12109.
[92] A.A. Alfadda, R.M. Sallam, Reactive oxygen species in health and disease, J. Biomed. Biotechnol. 2012 (2012), https://doi.org/10.1155/2012/936486.
[93] H. Wen, W.J. Xu, X. Jin, S. Oh, C.H.D. Phan, J. Song, S.K. Lee, S. Park, The roles of IP3 receptor in energy metabolic pathways and reactive oxygen species homeostasis revealed by metabolomic and biochemical studies, Biochim. Biophys. Acta - Mol. Cell Res. 2015 (1853) 2937–2944, https://doi.org/10.1016/j.bbamcr.2015.07.020.
[94] E. Villa, E. Proïcs, C. Rubio-Patiño, S. Obba, B. Zunino, J.P. Bossowski, R. M. Rozier, J. Chiche, L. Mondragón, J.S. Riley, S. Marchetti, E. Verhoeyen, S.W. G. Tait, J.E. Ricci, Parkin-independent mitophagy controls chemotherapeutic response in cancer cells, Cell Rep. 20 (2017) 2846–2859, https://doi.org/10.1016/j.celrep.2017.08.087.
[95] M.F. Chesselet, Dopamine and Parkinson's disease: is the killer in the house? Mol. Psychiatry 8 (2003) 369–370, https://doi.org/10.1038/sj.mp.4001289.
[96] E.F. Griffin, X. Yan, K.A. Caldwell, G.A. Caldwell, Distinct functional roles of Vps41-mediated neuroprotection in Alzheimer's and Parkinson's disease models of neurodegeneration, Hum. Mol. Genet. 27 (2018) 4176–4193, https://doi.org/10.1093/hmg/ddy308.
[97] P.A.C. Todd, H.V. McCue, L.P. Haynes, J.W. Barclay, R.D. Burgoyne, Interaction of ARF-1.1 and neuronal calcium sensor-1 in the control of the temperature-dependency of locomotion in Caenorhabditis elegans, Sci. Rep. 6 (2016) 1–12, https://doi.org/10.1038/srep30023.
[98] M.X. Wang, X.Y. Cheng, M. Jin, Y.L. Cao, Y.P. Yang, J. Da Wang, Q. Li, F. Wang, L. F. Hu, C.F. Liu, TNF compromises lysosome acidification and reduces α-synuclein degradation via autophagy in dopaminergic cells, Exp. Neurol. 271 (2015) 112–121, https://doi.org/10.1016/j.expneurol.2015.05.008.
[99] C.M. Lakhani, M.J.S. Benjamin, M. Davis, Glen F. Rall, 乳鼠心肌提取 HHS public access, Physiol. Behav. 176 (2017) 139–148, https://doi.org/10.1007/978-94-024-1088-4.
[100] L. Ji, H.T. Wu, X.Y. Qin, R. Lan, Dissecting carboxypeptidase E: properties, functions and pathophysiological roles in disease, Endocr. Connect. 6 (2017) R18–R38, https://doi.org/10.1530/EC-17-0020.
[101] N.P. Alza, P.A. Iglesias González, M.A. Conde, R.M. Uranga, G.A. Salvador, Lipids at the crossroad of α-synuclein function and dysfunction: biological and pathological implications, Front. Cell. Neurosci. 13 (2019) 1–17, https://doi.org/10.3389/fncel.2019.00175.
[102] J. He, M. Xia, P.K.K. Yeung, J. Li, Z. Li, K.K. Chung, S.K. Chung, J. Xia, PICK1 inhibits the E3 ubiquitin ligase activity of parkin and reduces its neuronal protective effect, Proc. Natl. Acad. Sci. U. S. A. 115 (2018) E7193–E7201, https://doi.org/10.1073/pnas.1716506115.
[103] Ann L. Coker, M.K. Nalawansha, Dhanusha A. Pflum, 乳鼠心肌提取 HHS public access, Physiol. Behav. 176 (2017) 139–148, https://doi.org/10.1038/nature18942.Rapid.
[104] D. Ryczko, R. Dubuc, Dopamine and the brainstem locomotor networks: from lamprey to human, Front. Neurosci. 11 (2017) 1–10, https://doi.org/10.3389/fnins.2017.00295.
[105] G. Stefanoni, G. Sala, L. Tremolizzo, L. Brighina, C. Ferrarese, Role of autophagy in Parkinson's disease, Autophagy Princ. Regul. Roles Dis. (2012) 243–264, https://doi.org/10.2174/092986732566180226094351.
[106] T.J.Van Ham, K.L. Thijssen, R. Breitling, R.M.W. Hofstra, R.H.A. Plasterk, E.A. A. Nollen, C. elegans model identifies genetic modifiers of α-synuclein inclusion formation during aging, PLoS Genet. 4 (2008), https://doi.org/10.1371/journal.pgen.1000027.
[107] P. Jadiya, S.S. Mir, A. Nazir, Effect of various classes of pesticides on expression of stress genes in transgenic C. elegans model of Parkinson's disease, CNS Neurol. Disord. Drug Targets 11 (2013) 1001–1005, https://doi.org/10.2174/18715273112110800009.
[108] T.D. Schmittgen, K.J. Livak, Analyzing real-time PCR data by the comparative CT method, Nat. Protoc. 3 (2008) 1101–1108, https://doi.org/10.1038/nprot.2008.73.
[109] M.B. Stocks, S. Moxon, D. Mapleson, H.C. Woolfenden, I. Mohorianu, L. Folkes, F. Schwach, T. Dalmay, V. Moulton, The UEA sRNA workbench: a suite of tools for analysing and visualizing next generation sequencing microRNA and small RNA datasets, Bioinformatics 28 (2012) 2059–2061, https://doi.org/10.1093/bioinformatics/bts311.
[110] S. Griffiths-Jones, R.J. Grocock, S. van Dongen, A. Bateman, A.J. Enright, miRBase: microRNA sequences, targets and gene nomenclature, Nucleic Acids Res. 34 (2006) 140–144, https://doi.org/10.1093/nar/gkj112.
[111] S.F. Altschul, W. Gish, W. Miller, E.W. Myers, D.J. Lipman, Basic local alignment search tool, J. Mol. Biol. 215 (1990) 403–410, https://doi.org/10.1016/S0022-2836(05)80360-2.
[112] S. Anders, W. Huber, Differential expression analysis for sequence count data, Genome Biol. 11 (2010) R106, https://doi.org/10.1186/gb-2010-11-10-r106.

ACS Medicinal Chemistry Letters

Letter

pubs.acs.org/acsmedchemlett

Discovery of 3-Arylcoumarin-tetracyclic Tacrine Hybrids as Multifunctional Agents against Parkinson's Disease

Koneni V. Sashidhara,*[,†] Ram K. Modukuri,[†] Pooja Jadiya,[‡] K. Bhaskara Rao,[†] Tanuj Sharma,[§] Rizwanul Haque,[‡] Deependra Kumar Singh,[§] Dibyendu Banerjee,[§] Mohammad Imran Siddiqi,[§] and Aamir Nazir[‡]

[†]Medicinal and Process Chemistry Division, [‡]Laboratory of Functional Genomics and Molecular Toxicology, and [§]Division of Molecular and Structural Biology, CSIR-Central Drug Research Institute, (CSIR-CDRI), BS-10/1, Sector 10, Jankipuram Extension, Sitapur Road, Lucknow 226031, India

Supporting Information

ABSTRACT: A series of multifunctional directed 3-arylcoumarin-tetracyclic tacrine derivatives was designed and synthesized for the treatment of Parkinson's disease (PD). A number of derivatives (**18**, **19**, **20**, **21**, and **24**) demonstrated significant reduction of aggregation of "human" alpha-synuclein (α-synuclein) protein, expressing on transgenic *Caenorhabditis elegans* (*C. elegans*) model NL5901. Moreover, compounds **16**, **18**, and **24** also exhibited good antioxidant properties and significantly increased the dopamine (DA) content in N2 and NL5901 strains of *C. elegans*. Interestingly, the protective efficacy of these hybrids seems to be mediated via activation of longevity promoting transcription factor DAF-16. In addition, molecular modeling studies have evidenced the exquisite interaction of most active compounds **18** and **24** with α-synuclein protein. Taken together, the data indicate that the derivatives may be useful leads against aging and age associated PD.

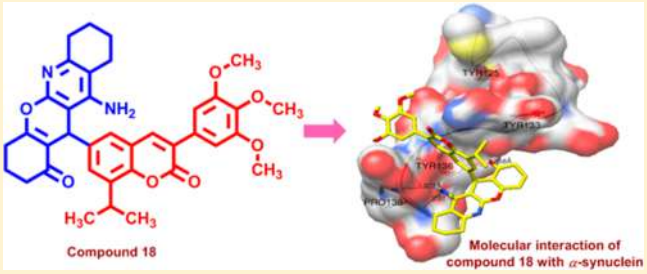

KEYWORDS: *3-Arylcoumarin, tetracyclic tacrine, Parkinson's disease, C. elegans, α-synuclein, reactive oxygen species*

Parkinson's disease (PD) is an irreversible neurodegenerative brain disorder, due to diminution of dopaminergic neurons in the region of substantia nigra.[1] The main pathological hallmark of PD is the presence and accumulation of a protein known as *alpha*-synuclein (α-synuclein).[2] The accumulation induces dopaminergic nerve terminal degeneration, which eventually leads to loss of dopamine-producing cells in the mid-brain.[3] In a disease condition, the gradual loss of dopamine levels leads to motor and nonmotor dysfunctions.[4] L-Dopa (levodopa) is the most potent medication used for over 30 years, which is the precursor of dopamine.[5] It effectively relieves the dopaminergic deficit; however, the disease persists and further uncontrolled symptoms leads to several complications like disturbing dyskinesias or unconditional movements.[6]

Presently, there is no cure for PD and the drugs used for treatment are mainly dopamine agonists (pramipexole and ropinirole) and monoamine oxidase inhibitors (rasagiline and selegiline) (Figure 1A), which provide only symptomatic relief.[7] Therefore, novel treatment and prevention approaches are urgently needed for PD therapy.

Because of the complex etiology found in PD, scientists are now turning to the design of multitarget-directed ligands (MTDLs) that should be able to interact with the multiple targets.[8] In the design of MTDLs, molecular hybridization strategy could be utilized, wherein two compounds binding to their targets are used as the starting points and their structural features are fused to incorporate activity at both targets into a single hybrid molecule.[9]

Considerable interest has been focused on the coumarin structure, which has been known to possess a broad spectrum of biological activities.[10] Recent evidence has suggested that 3-aryl coumarin nucleus constitutes a promising scaffold for inhibition of acetylcholinesterase (AChE) and AChE-induced β-amyloid aggregation.[11] Recently, Abdelhafez et al. reported that some of the 3-substituted coumarin derivatives potentially act as a dopamine releasing agent.[12] Other relevant reports have also suggested that these derivatives protect the neurons from the oxidative disorders and effectively enhance the dopamine biosynthesis.[13,14] However, the AChE inhibitors like donepezil and tacrine derivatives (Figure 1B) have shown beneficial effects in the treatment of PD.[15] Marco-Contelles et al. reported the neuroprotective activity of tetracyclic tacrine derivatives.[16] Some of recent reports have also underscored the importance of tacrine containing derivatives that could exhibit neuroprotective effects in an neurodegenerative condition.[17] The increase of the dopamine levels and decrease of ROS and neuroprotective properties are crucial to overcome PD. The concept of MTDL approach prompted us to synthesize a novel

Received: May 28, 2014
Accepted: August 20, 2014
Published: August 20, 2014

   dx.doi.org/10.1021/ml500222g | *ACS Med. Chem. Lett.* 2014, 5, 1099−1103

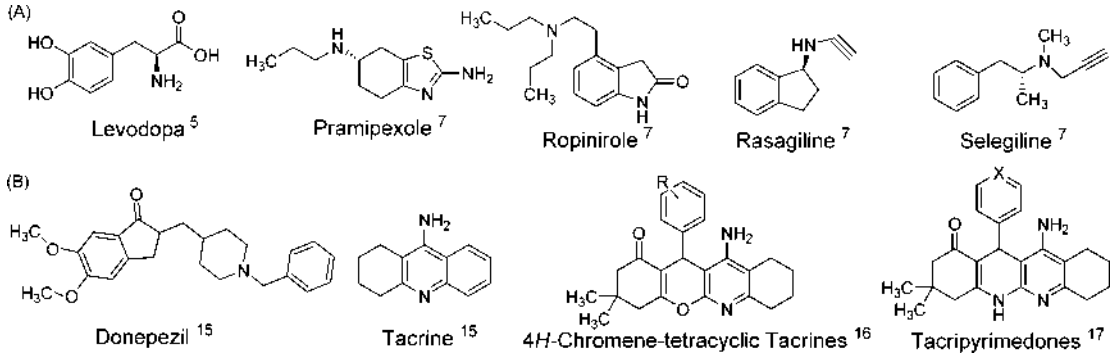

Figure 1. (A) Chemical structure of some potent anti-Parkinson's drugs. (B) Chemical structure of acetylcholinesterase inhibitors and some potent neuroprotective tetracyclic tacrine derivatives.

class 3-aryl coumarin and tetracyclic-tacrine hybrids that inhibit α-synuclein aggregation and increase availability of dopamine levels, thereby halting the progression of the disease.

The synthesis of target and intermediate compounds is represented in Scheme 1. The Duff formylation on different ortho-substituted phenols (**1** and **2**) in the presence of hexamethylenetetraamine (HMTA) and trifluoroacetic acid (TFA) at 120 °C gave aromatic dicarbaldehyde intermediates (**3** and **4**).[18] These dicarbaldehydes were then engaged with different substituted phenylacetic acids in the presence of cyanuric chloride and *N*-methyl morpholine (NMM) in DMF for 1 h, resulting in a good yield of respective 3-aryl coumarin aldehydes (**5**–**9**).[19] Further, these substrates (**5**–**9**) underwent the multicomponent reaction with malononitrile and different 1,3-cyclohexadiones in the presence of dimethylaminopyridine (DMAP) as a catalyst afforded coumarin-4*H*-chromene intermediates (**10**–**15**).[20] Finally, the Friedlander reaction between these intermediates (**10**–**15**)[21] and different cyclic ketones (cyclopentanone and cyclohexanone) in the presence of aluminum trichloride ($AlCl_3$) as a catalyst furnished the target 3-arylcoumarin-tetracylic tacrine derivatives (**16**–**24**) in good yields.

Scheme 1. Synthesis of 3-Arylcoumarin-tetracyclic Tacrine Derivatives[a]

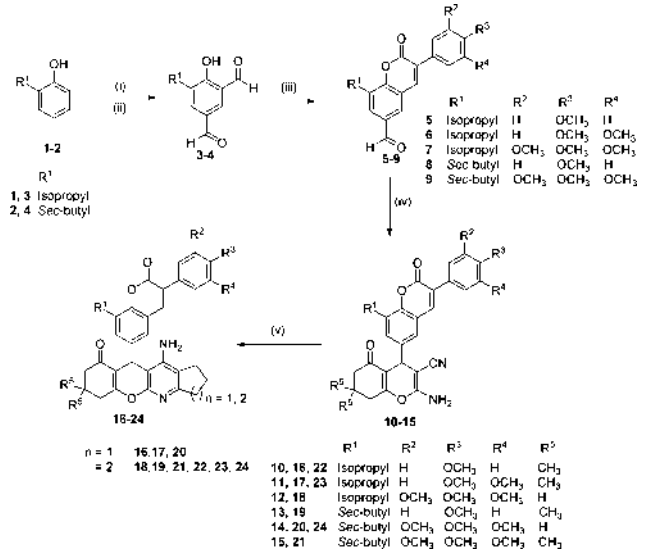

[a]Reagents and conditions: (i) HMTA, TFA, 120 °C, 4 h. (ii) aq. H_2SO_4, 100 °C, 2 h. (iii) Appropriate phenylacetic acid, cyanuric chloride, NMM, DMF, 110 °C, 30–90 min. (iv) Malononitrile, different 1,3-cyclohexadiones, DMAP, EtOH, reflux, 0.5 h. (v) Different cyclohexanones, $AlCl_3$, dichloroethane, reflux, 6 h.

In the present study, we utilized the transgenic *C. elegans* model to evaluate the effect of these compounds (racemic mixtures) on PD. The transparent anatomy of the nematode readily helps in monitoring the aggregation of the neural protein α-synuclein.[22] Interestingly, 60–80% of *C. elegans* genes are homologous to humans.[23]

We employed transgenic *C. elegans* model NL5901 expressing human α-synuclein protein tagged with yellow fluorescent protein (NL5901 (Punc-54::α- synuclein::YFP +unc-119)) in the body wall muscle.[24] We explored the role of different 3-arylcoumarin-tetracyclic tacrine derivatives on α-synuclein aggregation and compared it with the known positive control *Bacopa monneiri* (**BM**).[25] Worms treated with different derivatives were analyzed using fluorescent microscopy. We further quantified the images for fluorescence intensity of α-synuclein aggregation using ImageJ software. Out of nine compounds tested, five compounds exhibited significant reduction of aggregation of α-synuclein protein along with the positive control **BM**. In the case of worms treated with test compounds, **18**, **19**, **20**, **21**, and **24** showed mean fluorescence intensity 2.94 ± 0.24, 3.82 ± 0.25, 4.42 ± 0.15, 5.73 ± 0.40, and 3.76 ± 0.23 arbitrary units, respectively, thereby showing potential reduction by 2.6 ($p < 0.001$), 2.0 ($p < 0.01$), 1.76 ($p < 0.001$), 1.35($p < 0.05$), and 2.1 ($p < 0.001$) folds, when compared to untreated worms, whereas **BM** exhibited 1.25-fold reduction of α-synuclein aggregation ($p < 0.001$) (Figure 2). The mean fluorescence intensity for control group was 7.76 ± 0.03 arbitrary units. However, worms treated with compounds **16**, **17**, and **23** exhibited no effect on α-synuclein aggregation and mean fluorescence intensity 8.63 ± 0.10 arbitrary units. From the results, it is clear that compounds **18**, **19**, **20**, **21**, and **24** reduced the α-synuclein protein aggregation, suggesting their therapeutic potential against PD.

Pathogenesis of PD is intimately associated with oxidative stress, which is due to ROS generated by dopamine metabolism, mitochondrial dysfunction, and neuroinflammation.[26] Since the reduction of oxidative stress is another crucial aspect in designing agents for PD treatment, we examined antioxidative properties of our hybrids by using a non-fluorescent dye dichlorodihydrofluorescein diacetate (H_2DCFDA) assay, in the wild-type N2 strain of *C. elegans*.[27] Interestingly, compounds **16**, **18**, and **24** showed significant reduction in oxidative stress to that of untreated worms,

dx.doi.org/10.1021/ml500222g | ACS Med. Chem. Lett. 2014, 5, 1099–1103

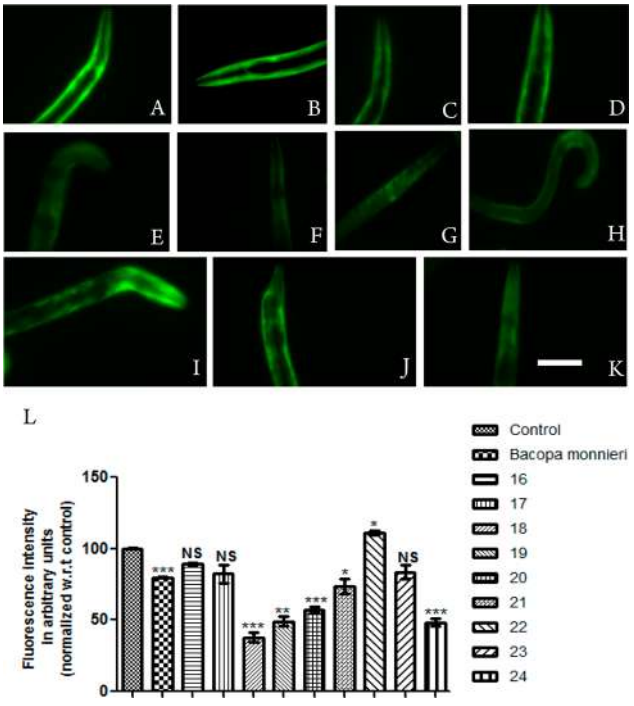

Figure 2. α-Synuclein aggregation in NL5901 strain of *C. elegans* treated with OP50 (A), *Bacopa monnieri* (B), **16** (C), **17** (D), **18** (E), **19** (F), **20** (G), **21**(H), **22** (I), **23** (J), and **24** (K). Scale bar, 50 μm. (L) Graphical representation for fluorescence intensity of aggregation of the nematodes as quantified using ImageJ software. *p < 0.05, **p < 0.01, ***p < 0.001, and NS, not significant.

suggesting that the hybrids have the potential to be potent multifunctional agents (Supporting Information Figure S1).

Since 3-arylcoumarin is a promising scaffold to inhibit AChE and AChE-induced β-amyloid aggregation,[11] we further examined the AChE inhibition property of these hybrids. In this study, we have employed an indirect method by the quantification of ACh level using amplex red assay kit. Worms treated with compounds **16**, **17**, **18**, **19**, **20**, **22**, **23**, and **24** except **21** exhibited a significant increase in the ACh level, indicating that the test compounds were significantly inhibiting AChE via increasing ACh level (Supporting Information Figure S2).

Among the various test compounds, **18** and **24** displayed the best effects in both reducing the α-synuclein aggregate and exhibiting antioxidant properties; therefore, **18** and **24** were taken further to analyze their effects on dopamine signaling. For the quantification of dopamine (DA) content, nonanol assay was employed, which gives us indirect readings of the DA contents as any deviation from the normal DA levels affects worm response time to volatile repellent nonanol.[28] Worms with higher DA content responds early by moving back, and the worm with decreased DA content takes longer time to respond toward nonanol. We quantified the effects of compounds **18** and **24** on the DA content along with **BM** in N2 and NL5901 strains of *C. elegans*.[29] After treatment of the worms with compounds **BM**, **18**, and **24**, the response time was significantly decreased by 1.63 (p < 0.05), 2.6 (p < 0.01), and 1.8 (p < 0.05) folds in N2 and 3.25 (p < 0.01), 1.75 (p < 0.05), and 1.9 (p < 0.05) folds in NL5901, respectively, as compared to untreated worms indicating that there was increase in DA content after treatment (Figure 3a). Thus, the DA content was improved considerably after exposure with **18** and **24** compounds in both the strains N2 and NL5901 of *C. elegans*.

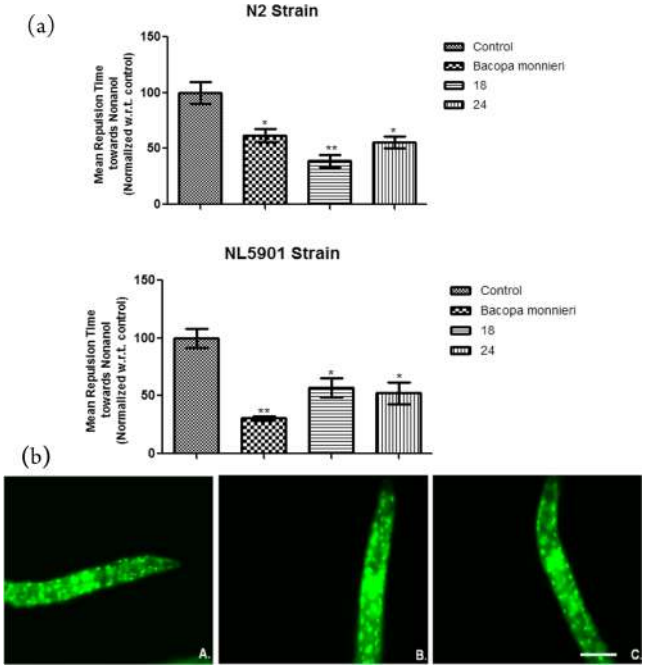

Figure 3. (a) Effect of active compounds on dopamine content as estimated by nonanol repulsion assay in N2 and NL5901 strain of *C. elegans*. *p < 0.05, **p < 0.01, NS, not significant. (b) DAF-16 expression in TJ356 strain of *C. elegans* fed with OP50 (A) and treated with compounds **18** (B) and **24** (C). Scale bar, 50 μm.

Since DAF-16 is considered as a major transcription factor required for the fundamental lifespan extension and longevity, its translocation into nucleus was examined by using a transgenic GFP expressing strain TJ356 of *C. elegans*.[30] An increase in GFP intensity was observed in the case of worms treated with compound **18** when compared to the worms raised on normal *E. coli*-OP50 diet. Figure 3b depicts the representative images for control (Figure 3b(A)), compound **18** treated worms (Figure 3b(B)), and compound **24** treated worms (Figure 3b(C)). However, no significant effect was observed in compound **24** treated worms as compared to the control. The present experiment suggested that the neuroprotective effects of compound **18** might be associated with DAF-16 signaling pathway.

Next, since tacrine derivatives are known to exhibit hepatotoxicity in liver, we examined the most active compounds for their cytotoxicities in Hep-G2 and HEK-293 cell lines. Interestingly, both the active compounds **18** and **24** possessed higher safety profile than tacrine (Supporting Information Figures S3 and S4).

The preceding experimental evidence on α-synuclein aggregation of these derivatives motivated us to probe the molecular interactions with α-synuclein protein for the most active compounds **18** and **24**. In the literature, docking studies of α-synuclein were successfully reported using Autodock 4.2 (Supporting Information Figure S5).[31] Autodock studies revealed that *S*-conformation of compound **18** (**18**-*S*) formed large clusters of 25 poses having least inhibitory constant (K_i) of 207.96 nM, binding energy of −9.12 kcal/mol, and displaying strong hydrogen bond by 1.858 Å with Tyr 136 and 1.973 and 2.077 Å hydrogen bonds with Pro138, indicating

dx.doi.org/10.1021/ml500222g | *ACS Med. Chem. Lett.* 2014, 5, 1099−1103

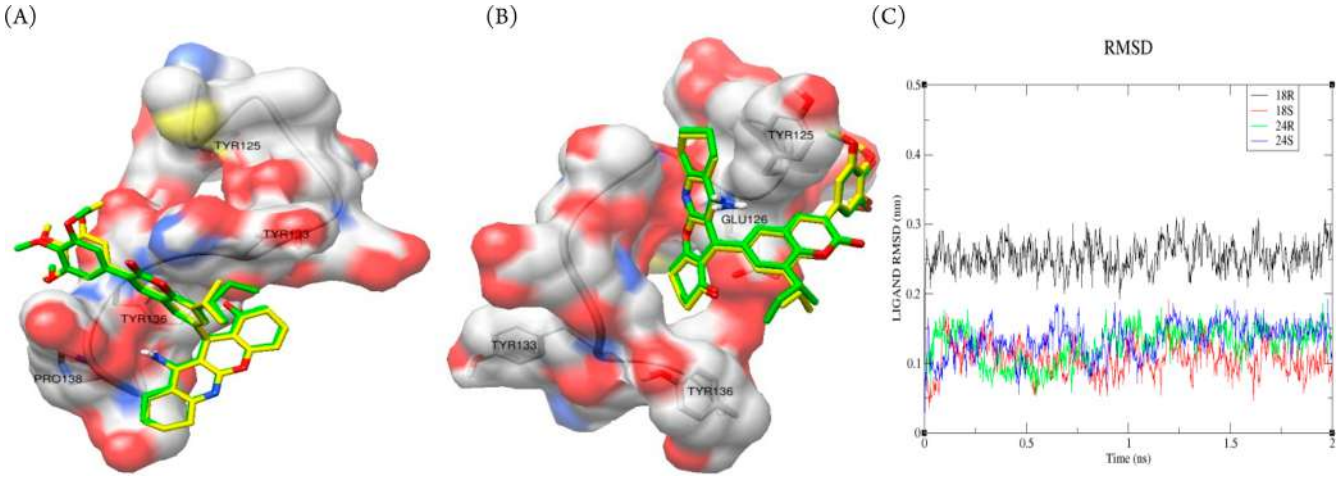

Figure 4. (A) Molecular interaction of compound **18**-*S* (yellow) and compound **24**-*S* (green) with α-synuclein. (B) Compound **18**-*R* (yellow) and compound **24**-*R* (green) with α-synuclein. (C) Temporal molecular dynamics studies of compounds **18**-*R*, **18**-*S*, **24**-*R*, and **24**-*S* for 2 ns.

interaction of ligand with tyrosine triad (Supporting Information Figure S6a). Thus, it can be used as an inhibitor for preventing α-synuclein aggregation and intracellular accumulation of misfolded protein. In the case of *S*-conformation of compound **24** (**24**-*S*), a cluster of 13 poses was formed having least K_i of 263 nM and binding energy of −8.98 kcal/mol. Compound **24**-*S*, in this lowest energy pose, shows a strong hydrogen bond by 1.806 Å with Tyr 136 and two hydrogen bonds of the order 1.845 and 2.078 Å with Pro138 (Supporting Information Figure S6b). Slight increase in K_i value of compound **24**-*S* compared to compound **18**-*S* can be attributed to its distorted trimethoxybenzene ring due to the presence of an extra methyl group, which is near to hydrophobic Tyr 133 (Figure 4A). Less number of poses in the least energy cluster size may possibly account for a slight decrease in activity of compound **24**-*S* compared to that of active compound **18**-*S*. Docking studies of the *R*-conformation of compounds **18** (**18**-*R*) and **24**-*R* reveal a potential binding site with lowest K_i value of 1.57 and 1.97 μM, respectively, both having hydrogen bond with Glu126 residue of the order 3.005 and 3.095 Å, respectively (Figure 4B and Supporting Information Figure S6c,d). In this study, the number of conformations in a simple cluster of compounds **18**-*R* and **24**-*R* were 45 and 28, respectively. Additionally, the molecular dynamics studies performed by Gromacs 4.5[32] indicated a stable binding of both isomers of **18** and **24** with root-mean-square deviation (rmsd) less than 0.3 nm over a time period of 2 ns (Figure 4C).[33]

In terms of preliminary structure−activity relationships of 3-arylcoumarin-tetracylic tacrine hybrids, compounds containing trimethoxy groups (**18**, **24**, **20**, and **21**) and alkyl substitution (*sec*-butyl and isopropyl group) at C8 position of 3-aryl coumarin ring are optimal for activity. However, on the tetracyclic tacrine core the presence of unsubstituted cyclohexanone and cyclohexane is preferred over substituted cyclohexanone and cyclopentane, respectively (**16** and **17**), in inhibiting the α-synuclein aggregation.

In conclusion, a series of novel multifunctional 3-arylcoumarin-tetracyclic tacrine derivatives have been synthesized and evaluated for PD therapy. Compounds **18** and **24** were identified as molecules of interest as they potentially inhibited the aggregation of α-synuclein protein and exhibited promising antioxidant properties. Interestingly, they also enhanced the dopamine content, which is crucial and beneficial for transporting signals to the nerve cells, in the condition of PD. Mechanistically, the protective efficacy of these derivatives seems to be mediated via signaling the expression of DAF-16 protein. Molecular modeling studies further corroborated and confirmed that compounds **18** and **24** strongly bind with the α-synuclein protein and efficiently inhibit the aggregation. Results presented herein not only reveal the structural and mechanistic insight of these novel hybrids but also provide impetus to synthesize enantiomerically pure molecules, which is ongoing in our lab.

■ ASSOCIATED CONTENT

Ⓢ Supporting Information

Experimental procedures, characterization of new compounds, and modeling and assay protocols. This material is available free of charge via the Internet at http://pubs.acs.org.

■ AUTHOR INFORMATION

Corresponding Author

*(K.V.S.) E-mail: kv_sashidhara@cdri.res.in or sashidhar123@gmail.com. Tel: +91 9919317940. Fax: +91-522-2771942.

Funding

R.K.M. and P.J. are thankful to CSIR, New Delhi, India for financial support. Nematode strains used in this work were provided by the *C. elegans* Genetics Center (CGC), University of Minnesota, MN, USA, which is funded by the NIH National Center for Research Resources (NCRR). This is CSIR-CDRI communication number 8763.

Notes

The authors declare no competing financial interest.

■ ACKNOWLEDGMENTS

Instrumentation facilities from SAIF and CDRI are gratefully acknowledged.

■ REFERENCES

(1) Obeso, J. A.; Rodriguez-Oroz, M. C.; Goetz, C. G.; Marin, C.; Kordower, J. H.; Rodriguez, M.; Hirsch, E. C.; Farrer, M.; Schapira, A. H.; Halliday, G. Missing pieces in the Parkinson's disease puzzle. *Nat. Med.* **2010**, *16*, 653−661.

(2) Spillantini, M. G.; Schmidt, M. L.; Lee, V. M.; Trojanowski, J. Q.; Jakes, R.; Goedert, M. Alpha-synuclein in Lewy bodies. *Nature* **1997**, *388*, 839−840.
(3) Lee, F. J.; Liu, F.; Pristupa, Z. B.; Niznik, H. B. Direct binding and functional coupling of alpha-synuclein to the dopamine transporters accelerate dopamine-induced apoptosis. *FASEB J.* **2001**, *15*, 916−926.
(4) Olanow, C. W.; Obeso, J. A.; Stocchi, F. Continuous dopamine-receptor treatment of Parkinson's disease: scientific rationale and clinical implications. *Lancet Neurol.* **2006**, *5*, 677−687.
(5) Lewitt, P. A. Levodopa for the treatment of Parkinson's disease. *N. Engl. J. Med.* **2008**, *359*, 2468−2476.
(6) Abbott, A. Levodopa: the story so far. *Nature* **2010**, *466*, S6−S7.
(7) Meissner, W. G.; Frasier, M.; Gasser, T.; Goetz, C. G.; Lozano, A.; Piccini, P.; Obeso, J. A.; Rascol, O.; Schapira, A.; Voon, V.; Weiner, D. M.; Tison, F.; Bezard, E. Priorities in Parkinson's disease research. *Nat. Rev. Drug Discovery* **2011**, *10*, 377−393.
(8) Morphy, R.; Rankovic, Z. Designed multiple ligands. An emerging drug discovery paradigm. *J. Med. Chem.* **2005**, *48*, 6523−6543.
(9) Cavalli, A.; Bolognesi, M. L.; Minarini, A.; Rosini, M.; Tumiatti, V.; Recanatini, M.; Melchiorre, C. Multi-target-directed ligands to combat neurodegenerative diseases. *J. Med. Chem.* **2008**, *51*, 347−372.
(10) Venugopala, K. N.; Rashmi, V.; Odhav, B. Review on natural coumarin lead compounds for their pharmacological activity. *Biomed. Res. Int.* **2013**, *2013*, 963248.
(11) Piazzi, L.; Rampa, A.; Bisi, A.; Gobbi, S.; Belluti, F.; Cavalli, A.; Bartolini, M.; Andrisano, V.; Valenti, P.; Recanatini, M. 3-(4-[[Benzyl(methyl)amino]methyl]phenyl)-6,7-dimethoxy-2*H*-2-chromenone (AP2238) inhibits both acetylcholinesterase and acetylcholinesterase-induced beta-amyloid aggregation: a dual function lead for Alzheimer's disease therapy. *J. Med. Chem.* **2003**, *46*, 2279−2282.
(12) Abdelhafez, O. M.; Amin, K. M.; Ali, H. I.; Maher, T. J.; Batran, R. Z. Dopamine release and molecular modeling study of some coumarin derivatives. *Neurochem. Int.* **2011**, *59*, 906−912.
(13) Matos, M. J.; Pérez-Cruz, F.; Vazquez-Rodriguez, S.; Uriarte, E.; Santana, L.; Borges, F.; Olea-Azar, C. Remarkable antioxidant properties of a series of hydroxy-3-arylcoumarins. *Bioorg. Med. Chem.* **2013**, *21*, 3900−3906.
(14) Yang, Y. J.; Lee, H. J.; Huang, H. S.; Lee, B. K.; Choi, H. S.; Lim, S. C.; Lee, C. K.; Lee, M. K. Effects of scoparone on dopamine biosynthesis and L-DOPA-induced cytotoxicity in PC12 cells. *J. Neurosci. Res.* **2009**, *87*, 1929−1937.
(15) Van Laar, T.; De Deyn, P. P.; Aarsland, D.; Barone, P.; Galvin, J. E. Effects of cholinesterase inhibitors in Parkinson's disease dementia: a review of clinical data. *CNS Neurosci. Ther.* **2011**, *17*, 428−441.
(16) Marco-Contelles, J.; León, R.; de los Ríos, C.; García, A. G.; López, M. G.; Villarroya, M. New multipotent tetracyclic tacrines with neuroprotective activity. *Bioorg. Med. Chem.* **2006**, *14*, 8176−8185.
(17) León, R.; de los Ríos, C.; Marco-Contelles, J.; Huertas, O.; Barril, X.; Luque, F. J.; López, M. G.; García, A. G.; Villarroya, M. New tacrine-dihydropyridine hybrids that inhibit acetylcholinesterase, calcium entry, and exhibit neuroprotection properties. *Bioorg. Med. Chem.* **2006**, *16*, 7759−7769.
(18) Sashidhara, K. V.; Kumar, M.; Khedgikar, V.; Kushwaha, P.; Modukuri, R. K.; Kumar, A.; Gautam, J.; Singh, D.; Sridhar, B.; Trivedi, R. Discovery of coumarin-dihydropyridine hybrids as bone anabolic agents. *J. Med. Chem.* **2013**, *56*, 109−122.
(19) Sashidhara, K. V.; Palnati, G. R.; Avula, S. R.; Kumar, A. Efficient and general synthesis of 3-aryl coumarins using cyanuric chloride. *Synlett* **2012**, *23*, 611−621.
(20) Khan, A. T.; Lal, M.; Ali, S.; Khan, M. M. One-pot three-component reaction for the synthesis of pyran annulated heterocyclic compounds using DMAP as a catalyst. *Tetrahedron Lett.* **2011**, *52*, 5327−5332.
(21) Marco-Contelles, J.; Pérez-Mayoral, E.; Samadi, A.; Carreiras, M. C.; Soriano, E. Recent advances in the Friedländer reaction. *Chem. Rev.* **2009**, *109*, 2652−2671.
(22) Bodhicharla, R.; Nagarajan, A.; Winter, J.; Adenle, A.; Nazir, A.; Brady, D.; Vere, K.; Richens, J.; O'Shea, P.; Bell, D. R.; de Pomerai, D. Effects of α-synuclein overexpression in transgenic *Caenorhabditis elegans* strains. *CNS Neurol. Disord. Drug Targets* **2012**, *11*, 965−975.
(23) Vistbakka, J.; VanDuyn, N.; Wong, G.; Nass, R. C. elegans as a genetic model system to identify Parkinson's disease-associated therapeutic targets. *CNS Neurol. Disord. Drug Targets* **2012**, *11*, 957−964.
(24) Shukla, V.; Phulara, S. C.; Yadav, D.; Tiwari, S.; Kaur, S.; Gupta, M. M.; Nazir, A.; Pandey, R. Iridoid compound 10-O-trans-p-coumaroylcatalpol extends longevity and reduces α synuclein aggregation in Caenorhabditis elegans. *CNS Neurol. Disord. Drug Targets* **2012**, *11*, 984−992.
(25) Jadiya, P.; Khan, A.; Sammi, S. R.; Kaur, S.; Mir, S. S.; Nazir, A. Anti-Parkinsonian effects of *Bacopa monnieri*: insights from transgenic and pharmacological *Caenorhabditis elegans* models of Parkinson's disease. *Biochem. Biophys. Res. Commun.* **2011**, *413*, 605−610.
(26) Dias, V.; Junn, E.; Mouradian, M. M. The role of oxidative stress in Parkinson's disease. *J. Parkinson's Dis.* **2013**, *3*, 461−491.
(27) Jadiya, P.; Nazir, A. Environmental toxicants as extrinsic epigenetic factors for Parkinsonism: Studies employing transgenic C. elegans model. *CNS Neurol. Disord. Drug Targets* **2012**, *11*, 976−983.
(28) Bargmann, C. I.; Hartwieg, E.; Horvitz, H. R. Odorant-selective genes and neurons mediate olfaction in *C. elegans*. *Cell* **1993**, *74*, 515−527.
(29) Kaur, S.; Sammi, S. R.; Jadiya, P.; Nazir, A. RNAi of cat-2, a putative tyrosine hydroxylase, increases alpha synuclein aggregation and associated effects in transgenic C. elegans. *CNS Neurol. Disord. Drug Targets* **2012**, *11*, 387−394.
(30) Chiang, W. C.; Tishkoff, D. X.; Yang, B.; Wilson-Grady, J.; Yu, X.; Mazer, T.; Eckersdorff, M.; Gygi, S. P.; Lombard, D. B.; Hsu, A. L. *C. elegans* SIRT6/7 homolog SIR-2.4 promotes DAF-16 relocalization and function during stress. *PLoS Genet.* **2012**, *8*, e1002948.
(31) Ruzza, P.; Siligardi, G.; Hussain, R.; Marchiani, A.; Islami, M.; Bubacco, L.; Delogu, G.; Fabbri, D.; Dettori, M. A.; Sechi, M.; Pala, N.; Spissu, Y.; Migheli, R.; Serra, P. A.; Sechi, G. Ceftriaxone blocks the polymerization of α-synuclein and exerts neuroprotective effects in vitro. *ACS Chem. Neurosci.* **2014**, *5*, 30−33.
(32) Hess, B.; Kutzner, C.; Van der Spoel, D.; Lindahl, E. GROMACS 4: algorithms for highly efficient, load-balanced, and scalable molecular simulation. *J. Chem. Theory Comput.* **2008**, *4*, 435−447.
(33) Huang, H. J.; Chen, H. Y.; Lee, C. C.; Chen, C. Y. Computational design of apolipoprotein e4 inhibitors for Alzheimer's disease therapy from traditional chinese medicine. *Biomed. Res. Int.* **2014**, *2014*, 452625.